agriculture

MDPI

Article

Candidate Pheromone Receptors of the Red-Belted Clearwing Moth *Synanthedon myopaeformis* Bind Pear Ester and Other Semiochemicals

Alberto Maria Cattaneo [1,*] and William B. Walker III [1,2]

[1] Chemical Ecology Group, Department of Plant Protection Biology, Swedish University of Agricultural Sciences, Box 190, Campus Alnarp, 234 22 Lomma, Sweden; william.walker@usda.gov
[2] Temperate Tree Fruit and Vegetable Research Unit, United States Department of Agriculture-Agriculture Research Service, Wapato, WA 98951, USA
* Correspondence: albertomaria.cattaneo@gmail.com

Abstract: The red-belted clearwing moth *Synanthedon myopaeformis* is a deleterious pest of apple orchards, wherein the larvae bore tree bark, resulting in reduced fitness and ultimately death. The main control strategies of this pest still rely on the use of pesticides, while alternative agronomic methods for its control coexist, with the application of the main pheromone (Z,Z)-3,13-octadecadien-1-yl acetate. Until now, the molecular bases of the chemosensory systems of the red-belted clearwing moth have been less explored. With the aim to identify novel ligands that may interfere with the behaviour of *S. myopaeformis*, in this study, we have isolated and functionally characterised some key odorant receptors (ORs) of this moth by selecting paralogues from two main subgroups of the Lepidopteran pheromone receptor (PR) clade: the OR3 subgroup (OR3.1 to OR3.4) and the OR22 subgroup (OR22.1 to OR22.4). We generated transgenic *D. melanogaster* expressing SmyoORs in ab3A neurons, which we approached by single sensillum recording (SSR). Among these ORs, we deorphanized SmyoOR3.4 to ligands that we have previously identified for orthologues of the codling moth *Cydia pomonella*, including the pear ester ethyl-(E,Z)-2,4-decadienoate, its methyl ester analogue methyl-(E,Z)-2,4-decadienote, and the unsaturated aldehyde (Z)-6-undecenal. With this approach, we also identified a wide pattern of activation of SmyoOR22.4 to several apple-emitted ligands. Despite the fact that combining SSR with gas chromatography (GC-SSR) did not unveil the activation of the SmyoORs to compounds present in the headspace from apples, GC-SSR unveiled the enhancement of the SmyoOR3.4 spiking at nanogram doses of both pear ester, methyl ester, and (Z)-6-undecenal. For the first time, this study deorphanized ORs from the red-belted clearwing moth and identified ligands as possible semiochemicals to add to the ongoing strategies for the control of this pest.

Keywords: the red-belted clearwing moth *Synanthedon myopaeformis*; odorant receptors (ORs); transgenic *Drosophila melanogaster*; single sensillum recording (SSR); gas-chromatographic SSR; functional characterization

Academic Editor: Long Zhang

Received: 14 March 2025
Revised: 14 May 2025
Accepted: 16 May 2025
Published: 21 May 2025

Citation: Cattaneo, A.M.; Walker, W.B., III. Candidate Pheromone Receptors of the Red-Belted Clearwing Moth *Synanthedon myopaeformis* Bind Pear Ester and Other Semiochemicals. *Agriculture* **2025**, *15*, 1112. https://doi.org/10.3390/agriculture15101112

Correction Statement: This article has been republished with a minor change. The change does not affect the scientific content of the article and further details are available within the backmatter of the website version of this article.

1. Introduction

The red-belted clearwing moth *Synanthedon myopaeformis* (Lepidoptera: Sesiidae) is a serious apple bark pest, native to Eurasia and North Africa [1] and currently diffused in North America [2]. Upon oviposition on apple barks, larvae of *S. myopaeformis* profit from size-controlled rootstocks, where burr knots have formed, to bore into the bark, causing a significant reduction in tree vigour and yield, until the destruction of the entire tree [3].

Several control strategies have been adopted to limit this pest, spreading beyond the most common use of broad-spectrum insecticides [4]. The impact of these chemicals on natural enemies [5,6] urged the implementation of integrated strategies such as the combination of growth regulators [7] or entomopathogenic nematodes [8]. Additional strategies involved bark barriers to limit the access of the insect by spreading cotton seed oil or using motor oil on the bark of the apple trees [9]. Other strategies involved selecting resistant apple rootstocks [10].

With the advent of semiochemical-based control strategies, several apple pest insects have been limited, enhancing the diversification of these methods towards multiple pest targets [11]. Since the end of the last century, a first chemical from the pheromone glands of the North American peach tree borer *Synanthedon exitiosa*, (Z,Z)-3,13-octadecadien-1-yl acetate [12], was identified as a strong sex-attractant for various Sesiid species of the genus *Synanthedon,* and has been selected among the most successful semiochemicals for the control of various among these bark borers [13–15].

Semiochemicals such as pheromone compounds are detected in the antennae of male moths by a dedicated population of olfactory sensory neurons (OSNs) expressing insect pheromone receptors (PRs). PRs are transmembrane proteins belonging to the odorant receptor (OR) family and, as ORs, they are co-expressed in OSNs together with the conserved co-receptor Orco [16,17], forming tetrameric structures working as ligand-gated ion channels [18], binding a wider (or narrower) spectrum of different ligands, with a combinatorial fashion: receptors vary widely in their breadth of tuning, and odorants vary widely in the number of receptors they activate [19].

With the aim to identify ligands active on insect ORs belonging to the PR clade, the use of transgenic *Drosophila melanogaster* represented a successful tool for achieving the deorphanization of the OR subunits from several insects, some of which belong to the order of Lepidoptera [20–22]. To this aim, the coding sequences of isolated insect ORs are expressed within empty neurons of *D. melanogaster* [23,24] by the use of the Gal4/UAS promoter system [25]. ORs form functional heteromers within the *D. melanogaster*'s empty neurons, together with the native odorant co-receptor. Empty neurons expressing heterologous ORs can be approached by following protocols for single sensillum recordings (SSRs) [26] aimed at identifying ligands active on the OR subunits.

Together with other successful approaches to study Lepidopteran pheromone receptors, in the last decade we have functionally expressed and characterised two key ORs that we have classified as members of the PR clade of the codling moth *Cydia pomonella* [27]: CpomOR3, which has a male and a female antennal bias, and is tuned to the pear ester ethyl-(E,Z)-2,4-decadienoate [28], and CpomOR22, which has a female antennal bias, and displays a wider tuning to various apple-emitted odorants, including alcohols, esters, but especially aldehydes and lactones [29].

The attractiveness of pear ester for the codling moth and the capacity of this kairomone to efficiently trap both males and females [30] have advanced various applications for both the monitoring and control of this pest [31–33]. Interestingly, field trials for this compound that aimed at monitoring the codling moth surprisingly resulted in trapping *S. myphaeformis* [34]. In accordance, the most recent findings from our labs also confirmed the emission of this compound from apples [35], linking the activity of both the codling moth and of *S. myopaeformis* to ecological relevance in apple orchards. The identification of additional ligands active on the chemosensory systems of the red-belted clearwing moth may be implemented in control strategies by adding novel semiochemicals to the ongoing methods that are mostly based on its pheromone.

Starting from a bioinformatic analysis of the *S. myopaeformis* male antennal transcriptome, in this study, we have identified a complex of four paralogues for both the OR3 and

the OR22 PRs of *S. myopaeformis*. Based on previous evidence from the activation of their orthologues from *C. pomonella* [28,29], this study claimed to functionally characterize OR3s and OR22s of *S. myopaeformis* through the screening of a few ligands, including the ones emitted from apples, and renowned as the most active on the ORs of the codling moth. We used the predicted coding sequences of SmyoORs to synthesize constructs and transform empty ab3A-neurons of *D. melanogaster*. Approaching transgenic *Drosophila* by SSR and coupling this technique with gas chromatography (GC-SSR), we deorphanize OR3s and OR22s paralogues of *S. myopaeformis*, which will lead the direction of efforts in search of novel ligands to implement interference with the behaviour of this moth.

2. Material and Methods

2.1. Insect Dissection and RNA Extraction

S. myopaeformis adult male insects were collected in 2016 from an apple orchard near Tordas, Hungary (GPS Coordinates: 47°21′42.8″ N 18°47′03.0″ E), with sex pheromone-baited sticky traps (CSALOMON, Plant Protection Institute, HUN-REN CAR, Budapest, Hungary). For dissections, one antenna was dissected from each of 100 wild-caught living males on the sticky traps. Using sharp forceps, antennae were removed at the base of the scape and immediately submerged in RNAlater (Sigma-Aldrich, St. Louis, MO, USA), and thereafter kept at 4 °C until shipment for RNA sequencing. The RNAlater samples were sent to LGC Genomics GmbH (Berlin, Germany) for further processing.

2.2. RNA Sequencing and Transcriptomics Analysis

Total RNA was extracted by LGC Genomics, and a cDNA library was prepared using standard in-house protocols. With Illumina MiSeq V3 and NextSeq 500 V2 sequencing, 300bp and 150 bp paired-end reads, respectively, were generated and saved in FASTQ format [36]. Pre-processing quality control of sequenced reads was carried out by LGC Genomics, as previously described [37]. A transcriptome comprised of the male antennae sequenced library was assembled using Trinity v.2.2.0 [38]; digitally normalised read pairs were used, all scaffolds larger than 200 bp were kept, and low confidence contigs were filtered out using RSEM v.1.2.14 [39]. To facilitate the unambiguous read mapping of sample reads to unique locations on the assembled transcriptome sequences for downstream quantitative analyses, the software CD-HIT-EST (v. 4.5.4-2011-03-07) was used to identify and remove redundant sequences that share 98% or greater identity with other sequences [40]. The transcriptome Trinity.fasta file was used as input, and program parameters -c 0.98 -n 8 were specified. In cases where sequences shared greater than 98% identity but were of different sizes, the largest of the sequences were retained in the fasta file.

BUSCO was used to assess the completeness of the male antennae transcriptome. For this, the Arthropoda and Lepidoptera orthologue databases, consisting of 1013 and 5286 core genes, respectively, that are highly conserved single-copy orthologs [41,42], were used to query the transcriptomes. For this process, the gVolante web server (https://gvolante.riken.jp/; accessed on 8 May 2025) was used with the following parameters: min_length_of_seq_stats: 1, assembly_type: trans, Program: BUSCO_v5, selected reference_gene_set: Arthropoda or Lepidoptera [43].

For the identification and characterization of *S. myopaeformis* odorant receptors (ORs), a text file was compiled in fasta format with OR protein sequences from our previously published *Cydia pomonella* olfactory transcriptome [27]. A BLAST nucleotide database was created from the Trinity.fasta file and was queried by the *C. pomonella* OR protein sequences by a tblastn search with BLAST v.2.9.0+ [44]. All BLAST hit transcripts were extracted from the Trinity.fasta file with an in-house script. Nucleotide sequences were translated into the protein sequence with the ExPASy web Translate tool (https://web.expasy.org/translate/;

accessed on 8 May 2025 [45]), and the protein sequences were aligned to *C. pomonella* reference annotations for confirmation with the ClustalOMEGA web tool (https://www.ebi.ac.uk/jdispatcher/msa/clustalo/; accessed on 8 May 2025 [46]).

The read mapping of sample reads to the de novo transcriptome and subsequent expression level abundance estimations were carried out, as described [47] with the Trinity Perl script "align_and_estimate_abundance.pl" Trinity v.2.8.4, using RSEM v.1.2.12 [39], Bowtie v.0.12.6 [48], and samtools v.0.1.19 [49]. A gene_trans_map file was generated with an RSEM perl script and used as input to assess relative expression levels for all transcripts within each relevant Trinity cluster. Estimated mapped reads for each gene were normalised by gene length to calculate fragments per kilobase per million reads (FPKM) values [39]. For the presentation of expression values, a heatmap plot was generated for the binary logarithm of raw FPKM values. Plots were made using the conditional formatting function in Microsoft Excel, with a three-colour scale. The minimum value was set to "lowest value", and displayed as white; the midpoint was set to "percentile", with a value of 75, and displayed as pink; the maximum was set to "highest value" and displayed as red. In the final format of the figure, the data were sorted from the highest value to the lowest value.

2.3. Phylogenetic Analysis of SmyoORs

For a comparative assessment of *S. myopaeformis* ORs contextualised to ORs from other lepidopteran species, phylogenetic analyses were performed on OR protein sequences, using the most complete version of the ORF determined from transcripts identified in this study (Supplementary Data File S1). Comparisons were made to OR repertoires from *Bombyx mori* [50,51], *Cydia pomonella* [52], and *S. littoralis* [53] (Supplementary Data File S2). All amino acid sequences were aligned using MAFFT online version 7.220 (https://mafft.cbrc.jp/alignment/server/, accessed on 21 February 2025) through the FFT-NS-I iterative refinement method, with JTT200 scoring matrix, "leave gappy regions" set, and other default parameters [54]. Aligned sequences were used to build the unrooted phylogenetic tree using PhyML 3.3 (http://www.atgc-montpellier.fr/phyml/; accessed on 21 February 2025) [55] using the BioNJ algorithm and maximum likelihood tree with Smart Model Selection (SMS) method [56], with the selection criterion set to the Bayesian Information Criterion. This software tool, which is integrated into the PhyML web server, automatically selects the best substitution model. In this analysis, the Q.pfam+R+F model was selected. For this model, equilibrium frequencies are ML optimised, the proportion of invariable sites is fixed at 0.0, and the number of free rate categories is 4. PhyML uses both NNI (nearest neighbour interchanges) and SPR (subtree pruning and regrafting) methods to rearrange and optimise the tree structure. Clade support for the maximum likelihood analysis was assessed using the Shimodiara–Hasegawa approximate likelihood ratio test (SH-aLRT) [57]. The nodes with support values SH-aLRT > 0.9 were considered well supported, nodes with values ranging from 0.8 to 0.9 were considered weakly supported, and node values < 0.8 were considered unsupported [55]. A consensus Newick format tree was visualised and processed in MEGA-11 software (version 11.0.10; [58]) and the final tree output was edited with Adobe Illustrator (version 28.7.1).

2.4. Cloning of Olfactory Receptors for Expression in the Drosophila Empty Neuron System

Synthetic constructs containing the complete ORFs encoding SmyoOR3.1, SmyoOR3.2, SmyoOR3.3, SmyoOR3.4, SmyoOR22.1, SmyoOR22.2, SmyoOR22.3, and SmyoOR22.4 as plasmid inserts in pCR2.1-Topo were obtained (Eurofins Genomics, Ebersberg, Germany). For each of these, the ORF was based upon the sequence identified in the transcriptome in this report, but was codon optimised for expression in *Drosophila melanogaster.* For

each gene, complete ORFs were amplified by PCR using full-length CDS primers (Supplementary Table S1), and the appropriate pCR2.1-Topo plasmid as the template. Purified PCR products were cloned into the PCR8/GW/TOPO plasmid (Invitrogen Life technologies, Grand Island, NY, USA). The integrity and the orientation of the insert was confirmed by Sanger sequencing 3730xl (Eurofins Genomics, Ebersberg, Germany). Cassettes with inserts were transferred from their TOPO/GW/PCR8 plasmids to the destination vector (pUASg-HA.attB, constructed by E. Furger and J. Bischof, kindly provided by the Basler group, Zürich, Switzerland), using the Gateway LR Clonase II kit (Invitrogen). The integrity and orientation of inserts was checked further by Sanger sequencing. Transformant *pUAS-SmyoOR3s* and *pUAS-SmyoOR22s* were generated by Best Gene (Chino Hills, CA, USA), using the PhiC31 integrase system. Briefly, recombinant pUASg-HA.attB-SmyoOR3 plasmids were injected into embryos of a *D. melanogaster* line containing an *attP* insertion site within the third chromosome (genotype y1 M{vas-int.Dm}ZH-2A w*; M{3xP3-RFP.attP}ZH-86Fb), leading to non-random integration. To drive the expression of SmyoOR3s and SmyoOR22s in the A neuron of ab3 basiconic sensilla (ab3A OSNs), *pUAS-SmyoOR3/OR22* lines were crossed to the Δ*halo*;*Or22a-Gal4* mutant line [23,24].

2.5. Single Sensillum Recordings (SSRs)

SmyoORs expressed in ab3A OSNs were tested through single sensillum recordings (SSRs). Three to eight-day-old flies were immobilised in 100 µL pipette tips with only the top half of the head protruding. The right antenna of each insect was gently pushed with a glass capillary tip against a glass support. The glass support and the capillary tip were fixed with dental wax on a microscope slide. Electrolytically sharpened tungsten electrodes (Harvard Apparatus Ltd., Edenbridge, UK) were used to penetrate the insect's body: the reference electrode was manually inserted in the right eye of the fly, while the recording electrode was maneuvered with a DC-3K micromanipulator equipped with a PM-10 piezo translator (Märzhäuser Wetzler GmbH, Wetzler, Germany) and inserted into ab3-sensilla. Signals coming from the olfactory sensory neurons were amplified 10 times with the INR-02 probe (Syntech, Hilversum, The Netherlands), digitally converted through an IDAC-4-USB interface (Syntech), and visualised and analysed with the software Autospike v. 3.4 (Syntech). To carry the odorant stimulus and prevent antennal dryness, a constant humidified flow of 0.65 m/s charcoal-filtered air was delivered through a glass tube and directed to the preparation.

To confirm the expression of SmyoOR-transgenes, the basic spiking of ab3-neurons were compared with the same parental fly Δ*halo*;*Or22a-Gal4* mutants that have been used to generate the offspring to be tested by SSR. Within a library of 27 odorant compounds available in our labs (Table 1), we included compounds based on our previous reports from emissions of apples [59], as well as pheromones and kairomones we have previously demonstrated as active ligands on ORs of the codling moth, including ligands for the orthologue *CpomOR3* [28,60]. The panel also included a renowned component of the sex pheromone of the genus *Synanthedon*: (Z,Z)-3,13-octadecadien-1-yl acetate (CAS: 53120-27-7; [61]). Based on the database of odorant responses (http://neuro.uni-konstanz.de/DoOR/content/DoOR.php; [62,63]), 2-heptanone (CAS 110-43-0) and 3-octanol (CAS: 589-98-0) were used as positive controls to validate recordings from ab3 sensilla by testing the activation of *D. melanogaster* ab3B. To discriminate ab3 from ab2 sensilla, the ab2A activator ethyl acetate (CAS: 141-78-6) was included as a negative control. To test absence in the ab3A neuron of the wild-type expression of OR22 subunits, ethyl hexanoate (CAS 123-66-0) was included as an additional negative control.

Table 1. Library of compounds screened against SmyoOR subunits, as indicated in methods. As a result of testing ligands, asterisks depict compounds enhancing significant ab3A spiking (Supplementary Data File S3); "i" depicts evidence of the sole inhibitory effect that we observed when testing (E,E)-8,10-dodecadien-1-ol on SmyoOR3.3.

Class	Compound Name	CAS	MW (g/mol)	Vp (mmHg @25 °C)	OR3.4	OR3.3	OR3.1	OR22.4	OR22.3	OR22.1
Alkane	Hexane	110-54-3	86.17758	151.000000				*		
Terpene alcohol	R-linalool	126-90-9	154.25266	0.091000				*		
Terpene alcohol	S-linalool	126-91-0	154.25266	0.091000				*		
Aromatic alcohol	2-phenylethanol	60-12-8	122.16690	0.086800				*		
Aliphatic alcohol	3-octanol	589-98-0	130.23066	0.512000		*	*			
Polyinsaturated alcohol	(E,E)-α-farnesol	4602-84-0	222.37142	0.000370				*		
Monoinsaturated alcohol	(Z)-3 hexen-1-ol	928-96-1	100.16084	1.039000	*			*		
Polyinsaturated alcohol	(E,E)-8,10-dodecadien-1-ol	33956-49-9	182.30654	0.001000		i		*		
Unsaturated aldehyde	nonanal	124-19-6	142.24166	0.532000				*		
Monoinsaturated aldehyde	(Z)-4-undecenal	68820-32-6	168.27960	0.045000	*			*		
Monoinsaturated aldehyde	(Z)-6-undecenal	-	168.27960	0.045400	*					
Polyinsaturated aldehyde	(E,E)-2,4-decadienal	25152-84-5	152.23672	0.030000	*			*		
Monoterpenoid aldehyde	Citral	5392-40-5	152.23672	0.200000				*		
Monoterpenoid aldehyde	β-cyclocitral	432-25-7	152.23672	0.176000				*		*
Aliphatic ketone	2-heptanone	110-43-0	114.18778	4.732000						
Fatty acid ester	Ethyl acetate	141-78-6	88.10616	111.716003						
Fatty acid ester	Ethyl hexanoate	123-66-0	144.21392	1.665000	*					
Aliphatic ester	Ethyl-(E,Z)-2,4-decadienoate	3025-30-7	196.28980	0.010000	*			*		
Aliphatic ester	Methyl-(E,Z)-2,4-decadienoate	4493-42-9	182.26286	0.028000	*			*		
Aliphatic ester	hexyl 2-methyl-butanoate	10032-15-2	186.29474	0.158000	*			*		
Aromatic ester	Methyl salicylate	119-36-8	152.14936	0.034300				*		
Polyinsaturated aliphatic acetate	(E,E)-8,10-dodecadien-1-yl acetate	53880-51-6	224.34368	0.001000				*		
Polyinsaturated aliphatic acetate	(Z,Z)-3,13-octadecadien-1-yl acetate	53120-27-7	308.50532	-				*		
Sesquiterpene	(E)-β-farnesene	18794-84-8	204.35628	0.010000	*			*		
Sesquiterpene	(E,E)-α-farnesene	502-61-4	204.35628	0.010000				*		
Sesquiterpene	(E)-β-caryophyllene	87-44-5	204.35628	0.013000				*		*
Aromatic nitrile	Phenylacetonitrile	140-29-4	117.15079	0.056000				*		
Alkatriene	4,8-dimethyl-1,3(E),7-nonatriene (DMNT)	19945-61-0	150.26446	-				*		

To screen the panel, odorants were diluted in hexane (Sigma Aldrich, St. Louis, MO, USA) at 1.0 µg/µL. Stimuli were prepared by applying 10.0 µL of each dilution on grade 1–20 mm circular filter paper (GE Healthcare Life Science, Little Chalfont, UK), previously inserted into glass Pasteur pipettes (VWR, Milan, Italy), for a total amount of 10.0 µg of compound per stimulus. Puffing provided an additional 2.5 mL of air through the pipette for 0.5 s, by inserting the pipette within a side hole of the glass tube, directing the humidified air flow to the antennae. To characterize the intensity of the response, the spike frequency was calculated by subtracting ab3A spikes that were counted for 0.5 s before the stimulus from the number of spikes that were counted for 0.5 s after the stimulus, with the aim of calculating the spike frequency in terms of Δspikes/0.5sec. For each receptor, responses to compounds of the panel were compared for five insects using a single insect as a replicate. Before validating significant differences in spike counting, tests of normality with the IBM SPSS Statistics software 29.0 (https://www.ibm.com/, accessed on 10 December 2023) unveiled that for some ligands, data were not normally distributed (Kolmogorov–Smirnova/Shapiro–Wilk test $p < 0.05$, Supplementary Data File S3). Using the same software, spike frequencies of each compound were compared, with respective values from the solvent (hexane) by the non-parametric Wilcoxon Signed Rank test ($p < 0.05$). For the box-plot analysis, Δspikes/0.5sec of each recording were normalised to the averaged ab3A firing rate for the specific insect replicate, as performed in our previous studies.

Dose–response experiments were conducted on SmyoOR3.4, which we have selected among the most active subunits. To perform dose–response experiments, we identified three key ligands that we have found active on SmyoOR3.4, including the pear ester (ethyl-E,Z-2,4 decadienoate, CAS: 3025-30-7, (E,Z)-ED) and methyl pear ester (methyl-E,Z-2,4 decadienoate, CAS: 4493-42-9, (E,Z)-MD) that we have previously reported to be the main activators of the codling moth orthologue CpomOR3 [28,60]. In addition, we selected an aldehyde available in our labs: (Z)-6-undecenal (Z6-11Al, CAS: unattributed), which we have found active only on SmyoOR3.4 and which unveiled the highest average in Δspikes/0.5sec among all the compounds we tested on this subunit (34.6 ± 6.9 Δspikes/0.5sec; Supplementary Data File S3).

To perform dose–response experiments, compounds were diluted in hexane between 0.1 µg/µL and 10 µg/µL, to prepare aliquots ranging from 1.0 to 150/200 µg on filter paper, depending on the experiment, using at most 15/20 µL of the dilution volume per stimulus. For each dose, the ab3A spike frequency for 0.5 seconds was doubled to calculate Δspikes/sec, and corrected accounting for differences in vapour pressure [64], taking (Z)-6-undecenal as the reference ligand, being the most active. To normalise for vapour pressure, we considered the reference value presently available for the (E)-6-undecenal geometric isomer (CAS: 60671-73-0; http://www.perflavory.com/episys/ps1118261.html) (Supplementary Data File S4). Dose-related effects were analysed by SigmaPlot 13.0 (Systat Software Inc., San Jose, CA, USA).

2.6. Gas Chromatography Coupled with Single Sensillum Recordings (GC-SSR)

GC-SSR was performed as previously described [65,66], testing doses of the aforementioned ligands (ethyl-E,Z-2,4 decadienoate, methyl-E,Z-2,4 decadienoate and (Z)-6-undecenal) on insects carrying the SmyoOR3.4 transgene. Doses ranged from 1.0 ng to 0.1 µg of active compounds, using the same equipment that we have optimised in previous research [29,65,66]. In brief, samples were injected on a 7890 GC-system (Agilent Technologies Inc., Santa Clara, CA, USA) with a 30 m × 0.32 mm fused silica capillary column (Agilent Technologies Inc.), coated with HP-5, df = 0.25 µm, programmed from 30 °C (hold 3 min) at 8 °C/min to 250 °C (hold 5 min) (software: GC-SSR-1—Agilent.OpenLab, Agilent Technologies). The outlet split from the GC column was a 1:1 ratio between the

flame ionization detector and the mounted antenna, according to instrument settings. A humidified flow of 3.5–4.0 L/min charcoal-filtered air was directed into a 90-degree-angled glass tube with a hole in the angle where part of the column exiting from the transfer line was accessed. Glass tubing was adjusted to a length of 17 cm, and ab3 sensilla was tested following the same optimisation to 1.0 nanogram of the active compound, which we have adopted in Cattaneo et al. [65]. The recording window was set to 35 min upon the preliminary observation of retention times for the injected compounds. Using GC-SSR, we tested 1.0 to 100.0 ng aliquots of ethyl-E,Z-2,4 decadienoate, methyl-E,Z-2,4 decadienoate, and (Z)-6-undecenal. Compounds were diluted in hexane between 0.001 and 0.100 µg/µL depending on the experiment condition, injecting 2.0 µL dilutions into the gas chromatograph. Parallel experiments tested SmyoOR3.4 and SmyoOR22.4 subunits using GC-SSR, injecting volatile collections from the apple headspace (Hoplomalus and *Malus*) already available in our labs, extracted by methods that we have recently published [29]. To test headspace collections, hexane-diluted aliquots of 4.0 µL were injected into the gas chromatograph. For comparative experiments, the same headspace has been tested on fly lines expressing CpomOR3 in ab3A neurons, already present in our stocks from previous studies [28,60]. The effects of CpomOR3 to the headspace were compared with hexane upon counting 5.0 sec from the start of the effect or from the release of hexane. Numbers were subtracted to spikes from 5.0 sec, anticipating the effect and divided by 5 to calculate Δspikes/sec. Normality was tested by SPSS performing a Kolmogorov–Smirnova/Shapiro–Wilk test ($p > 0.05$), which informed the statistical analysis using a paired *t*-test (Supplementary Data File S3). The comparison with authentic samples was performed by testing CpomOR3 by injecting a mixture of 2.0 µL of a blend containing 5.0 ng/µL ethyl-E,Z-2,4 decadienoate, methyl-E,Z-2,4 decadienoate, and (Z)-6-undecenal.

2.7. Sequence and Structural Analysis

Polypeptide sequences of CpomOR3 (GenBank: AFC91713.2) and translated ORFs of SmyoOR3.4, SmyoOR3.3, SmyoOR3.2, and SmyoOR3.1 were aligned by muscle (https://www.ebi.ac.uk/jdispatcher/msa/muscle, using the ClustalW format to generate sequence alignment [67]. As carried out in previous studies [65,68], transmembrane domains for OR3 proteins were predicted with Topcons (http://topcons.cbr.su.se/ [69]). The topology for transmembrane domains was predicted using Protter V. 1.0 (http://wlab.ethz.ch/protter/ [70]). The results from Multalin and Protter were elaborated using Affinity Designer 1.10.6.1665. Given the absence of a deposited 3D structure for SmyoOR3.4, we used the *C. pomonella* CpomOR3 as a model to simulate 3D analysis, by downloading the respective PDB accession (UniProt H9A5M3) from AlphaFold (https://alphafold.ebi.ac.uk/) that we submitted and edited using RasTop (https://www.geneinfinity.org/rastop/). Because of the absence of deposited OR22 structures of the orthologues from species of the genus *Synanthedon*, *C. pomonella*, and other Lepidopterans [27], the 3D analysis of OR22s was not conducted.

3. Results

3.1. Phylogenetic Analysis and Relative Expression of SmyoORs

A whole-tissue transcriptome was generated from total RNA extracted from *S. myopaeformis* male antennae. In total, 237,934 transcripts (>201 nucleotides) were assembled, with a mean length of 639 nts, an N50 of 843, and 33,996 sequences greater than 1000 nts (Supplementary Data File S5). BUSCO completeness assessment revealed hits for 98.12% of 1013 core genes (with 95.06% complete) from the Arthropoda orthologue set, and 87.31% of 5286 core genes (with 82.80% complete) from the Lepidoptera orthologue set (Supplementary Data File S5). These findings suggest a satisfactory level of completeness for the

transcriptome and indicate that the assessment of the degree of completeness may vary depending upon which orthologue set is used.

The analysis of transcripts that encode candidate ORs revealed at least 62 OR genes expressed in male antennae, with 65 potential candidate proteins identified, including three hypothetical isoforms (SmyoOR19a/b, SmyoOR28a/b, SmyoOR53a/b). Of these, 55 are predicted to contain complete open reading frames, encoding the entire functional protein (Supplementary Data File S1). A phylogenetic analysis was conducted, comparing candidate ORs to repertoires from other lepidopteran species (*B. mori*, *C. pomonella*, and *S. littoralis*) to provide evolutionary context and facilitate functional hypotheses for individual genes. *S. myo* ORs displayed distributions across all major clades of lepidopteran ORs. Notably, within the canonical pheromone receptor clade, nine predicted ORs were identified. These clustered entirely within the subfamilies inclusive of either CpomOR3 or CpomOR22 (Figure 1).

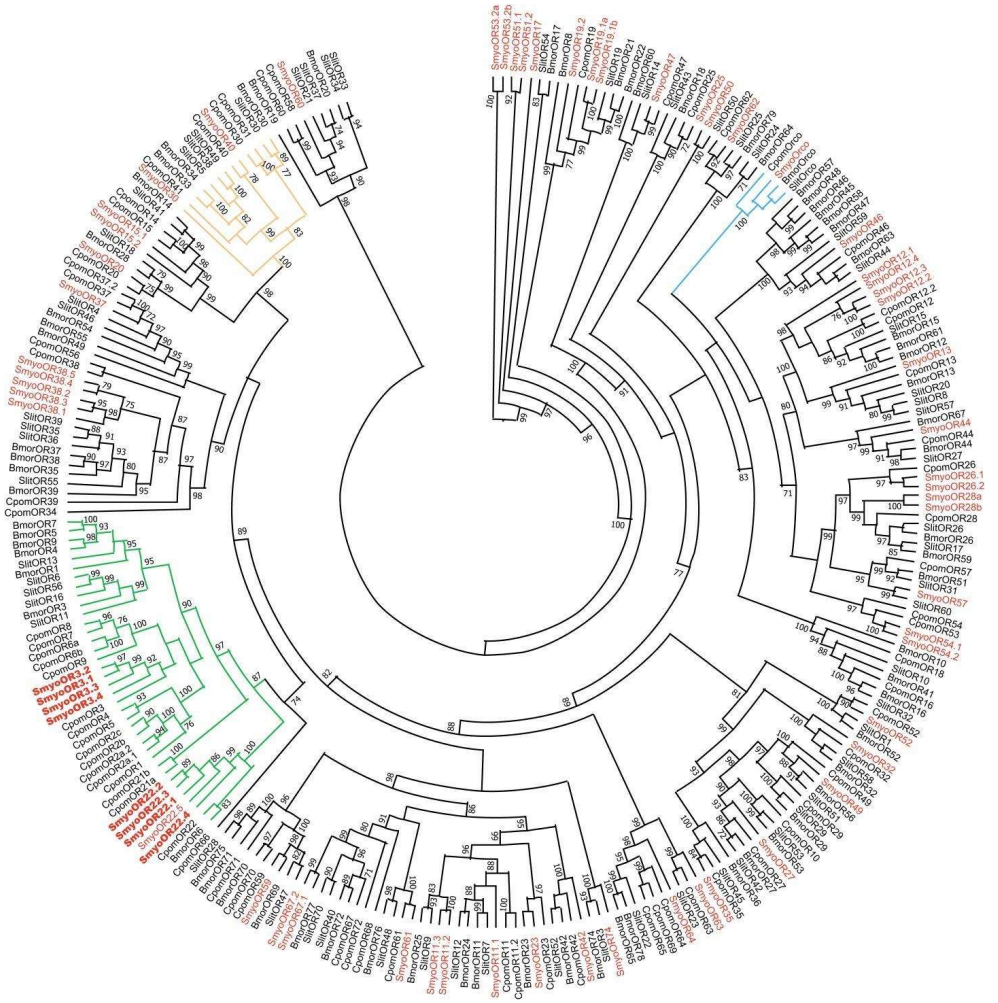

Figure 1. Maximum likelihood phylogenetic tree of candidate SmyoOR sequences with other lepidopteran OR sequences. Unrooted phylogenetic tree built using the online tool PhyML 3.0. Includes sequences from *Bombyx mori* (Bmor), *Cydia pomonella* (Cpom), and *Spodoptera littoralis* (Slit). Branches of the Orco clade are coloured light blue; branches of the lepidopteran canonical "Pheromone Receptor" clade are coloured green; branches of the expanded novel pheromone receptor clade are coloured orange; *S. myopaeformis* ORs are indicated with red font and those functionally studied in this report are marked with bold font. Node support was assessed with the Shimodiara–Hasegawa approximate likelihood ratio test (SH-aLRT); values greater than 0.7 are shown.

Abundance estimates were calculated for all candidate ORs. Consistent with other studies, the odorant receptor co-receptor, Orco, was the most highly expressed OR gene, with an FPKM of 176.04. Among non-Orco ORs, SmyoOR54.1 (44.23 FPKM), SmyoOR62 (38.34 FPKM), SmyoOR22.1 (36.3 FPKM), and SmyoOR22.3 (29.96 FPKM) were the most abundantly expressed ORs (Figure 2; Supplementary Data File S6). Based upon phylogenetic clustering of the OR3 and OR22 candidate homologues within the canonical pheromone receptor clade and relatively high expression of several of these genes in male *S.myopaeformis* antennae, SmyoOR3.1-OR3.4 and SmyoOR22.1-OR22.4 were selected for the functional characterization analysis.

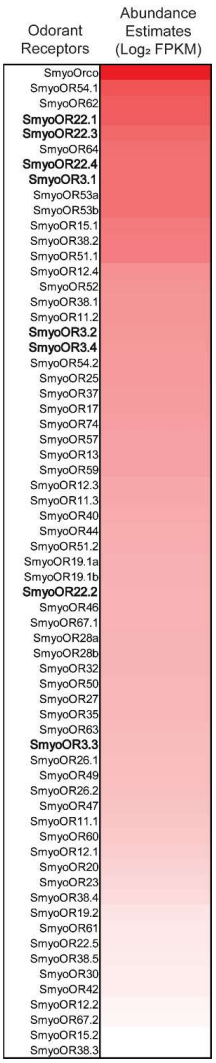

Figure 2. Heat plot of relative expression values for *Synanthedon myopaeformis* odorant receptors (ORs). Estimation of abundance values determined by read mapping. Receptors are sorted according to decreasing abundance: white and lighter pink colours indicate relatively lower expression, darker pink and red indicate relatively higher expression. Colour plots represent binary log of FPKM for each gene (See Supplementary Data File S6 for raw data). A larger bold font is used to indicate ORs functionally examined in this report. Range of values for male antenna: 0.44–7.46.

3.2. Functional Characterization and Activation of SmyoORs

The confirmation of the expression of an OR transgene in the progeny generated from crossing *pUAS-SmyoOR3* lines with Δ*halo;OR22a-Gal4* mutants (w;Δ*halo*;pUAS-SmyoOR3/*p22a-Gal4*) was demonstrated by the recovery of an ab3A spiking phenotype, absent among parental Δ*halo;OR22a-Gal4* insects, as reported from previous studies based on the use of transgenic *Drosophila* [23,65] (Figure 3A).

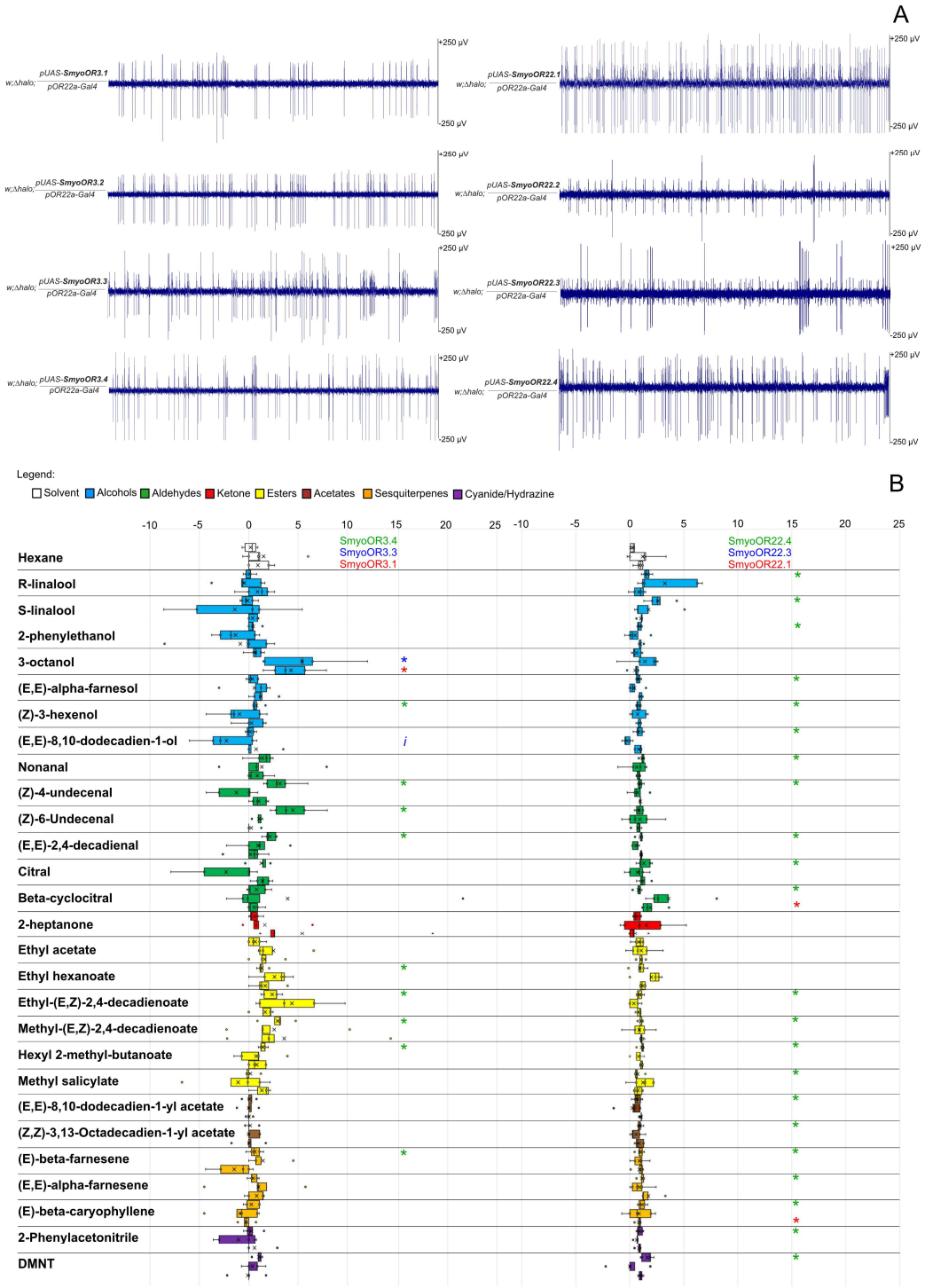

Figure 3. Functional expression of SmyoOR subunits. (**A**) Basic spiking of SmyoOR subunits. Note: expression of SmyoOR3.2 and SmyoOR22.2 unveiled absence of spiking. (**B**) Box-plot analysis of

ab3A spiking for SmyoOR3- (**left**) and SmyoOR22subunits (**right**) from transgenic *D. melanogaster* expressing SmyoORs in ab3A neurons, when tested with the compound library from Table 1. Asterisks indicate compounds enhancing significant differences in spiking when compared with the solvent (Wilcoxon Signed Rank test: $p < 0.05$; N = 5). Asterisks' colours refer to specific subunits as SmyoOR3.4/OR22.4 (green), SmyoOR3.3/OR22.3 (blue) and SmyoOR3.1/OR22.1 (red). As in Table 1, "i" depicts evidence of the sole inhibitory effect that we observed when testing (E,E)-8,10-dodecadien-1-ol on SmyoOR3.3.

Among the eight SmyoOR subunits that we have tested, we observed a significant difference in spiking when insects were stimulated with various compounds from the panel (Table 1). The SmyoOR3.4 and SmyoOR22.4 subunits were observed to be the most active, SmyoOR3.3, OR3.1, and OR22.1 responded to few ligands, SmyoOR3.2 and OR22.2 were inactive, and OR22.3 was unresponsive to any tested compound (Table 1, Figure 3B, Supplementary Data File S3). Interestingly, out of the two ligands active on SmyoOR3.3, (E,E)-8,10-dodecadien-1-ol was inhibitory (0.40 ± 4.55 Spikes/0.5sec). By observing an overall lack of ab3A spiking when we tested SmyoOR3.2 and SmyoOR22.2 (Figure 3A), we decided to not perform a further analysis for these subunits (Supplementary Data File S3).

3.3. Dose–Response Experiments

The comparison of dose–response characteristics and their related kinetic parameters for SmyoOR3.4, after adjustment to vapour pressure (Figure 4A), resulted in the following sensitivity equation: $EC50_{(E,Z)\text{-}MD}$ (6.661 ± 0.6598 μg) < $EC50_{Z6\text{-}11Al}$ (8.140 ± 3.267 μg) < $EC50_{(E,Z)\text{-}ED}$ (8.807 ± 1.573 μg), with respective Hill coefficients h ~ 4.318 ± 1.699 [(E,Z)-MD]; 1.784 ± 1.582 [Z6-11Al]; 1.992 ± 0.8286 [(E,Z)-ED] and different amplitudes (Fmax ~ 101.40 ± 6.228 Δspikes/sec [(E,Z)-MD]; 115 ± 15.53 Δspikes/sec [Z6-11Al] and 296 ± 22.61 Δspikes/sec [(E,Z)-ED]), resulting in the highest amplitude for pear ester. Upon normalisation to the respective saturating doses [(E,Z)-MD, 50 μg; Z6-11Al, 50 μg; (E,Z)-ED, 100 μg] the analysis of dose–response characteristics resulted in the following parameters: $EC50_{(E,Z)\text{-}MD}$ (6.716 ± 0.5966 μg) < $EC50_{Z6\text{-}11Al}$ (7.243 ± 3.381 μg) < $EC50_{(E,Z)\text{-}ED}$ (8.019 ± 0.8927 μg); Hill coefficients h ~ 4.463 ± 1.605 [(E,Z)-MD]; 1.596 ± 1.512 [Z6-11Al]; 3.300 ± 1.408 [(E,Z)-ED]; Fmax ~ 0.8903 ± 0.0505 Δspikes/(sec)spikes [(E,Z)-MD]; 0.838 ± 0.1286 Δspikes/(sec)spikes [Z6-11Al] and 0.8739 ± 0.05512 Δspikes/(sec)spikes [(E,Z)-ED]. The dose–response analysis performed using SSR suggested that (E,Z)-ED was the main agonist, and (E,Z)-MD and Z6-11Al were partial agonists.

Conversely, GC-SSR, which we approached as an alternative method for the dose–response analysis, demonstrated activation at lower doses of these three compounds (100 ng; Figure 4B), unveiling evident effects proximal to 1.0 ng solely for (Z)-6-undecenal, while effects by injecting (E,Z)-ED and (E,Z)-MD were visible starting from higher doses.

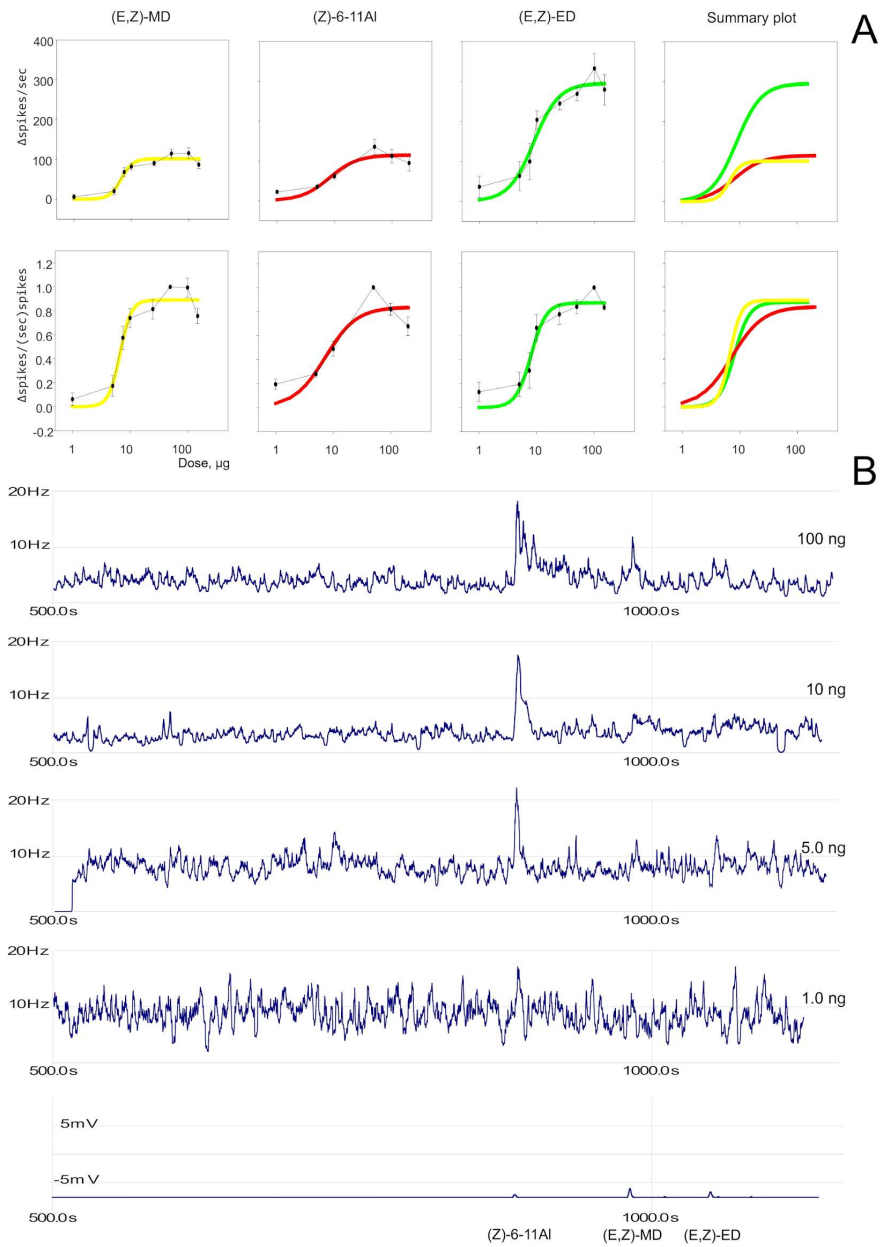

Figure 4. Dose–response and GC-SSR analysis of selected SmyoOR3.4-active ligands. (**A**) Dose–response characteristics of SmyoOR3.4 when tested to methyl (E,Z)-2,4 decadienoate, (Z)-6 undecenal and ethyl (E,Z)-2,4 decadienoate upon adjustment to vapour pressure. Below: normalised effect to the respective saturating doses. Right: summary plots. (**B**) Gas chromatography-coupled single sensillum recording (GC-SSR) traces of a blend containing (Z)-6-undecenal [Z6-11Al], methyl (E,Z)-2,4-decadienoate [(E,Z)-MD] and ethyl (E,Z)-2,4-decadienoate [(E,Z)-ED] at doses ranging between 1.0 and 100 ng. Note: for (Z)-6-undecenal, effects are evident from doses proximal to 5.0 ng, for (E,Z)-MD from 10.0 ng, and for (E,Z)-ED from 100 ng. Below: the GC spectrum indicated peaks associated with 5.0 ng doses (GC 10 mV). Frequency plot (SSR 20 Hz) represents ab3A spikes per second, set with a Bin width of 100 ms seconds and a smooth filter line with 25 Taps.

3.4. GC-SSR Testing Headspace Collections

The headspace from Hoplomalus and *Malus* unveiled an absence of effects when tested on SmyoORs (Supplementary Figure S1). Conversely, most of the headspace samples that we have tested demonstrated effects on fly lines expressing CpomOR3 in ab3A sensilla in proximity of a GC peak associated with a retention time of 1055 s (Figure 5A, Supplementary Data File S3). A comparison with authentic samples that we selected from our panel (Table 1)

based on our previous findings demonstrated that this effect matched the same retention time of the pear ester ethyl-(E,Z)-2,4-decadienoate. Note: this is the sole retention time in the GC spectrum that we have found to be active when testing the headspace on CpomOR3 as evidence of the possible presence of this ligand in the Hoplomalus and *Malus* headspace (Supplementary Data File S3).

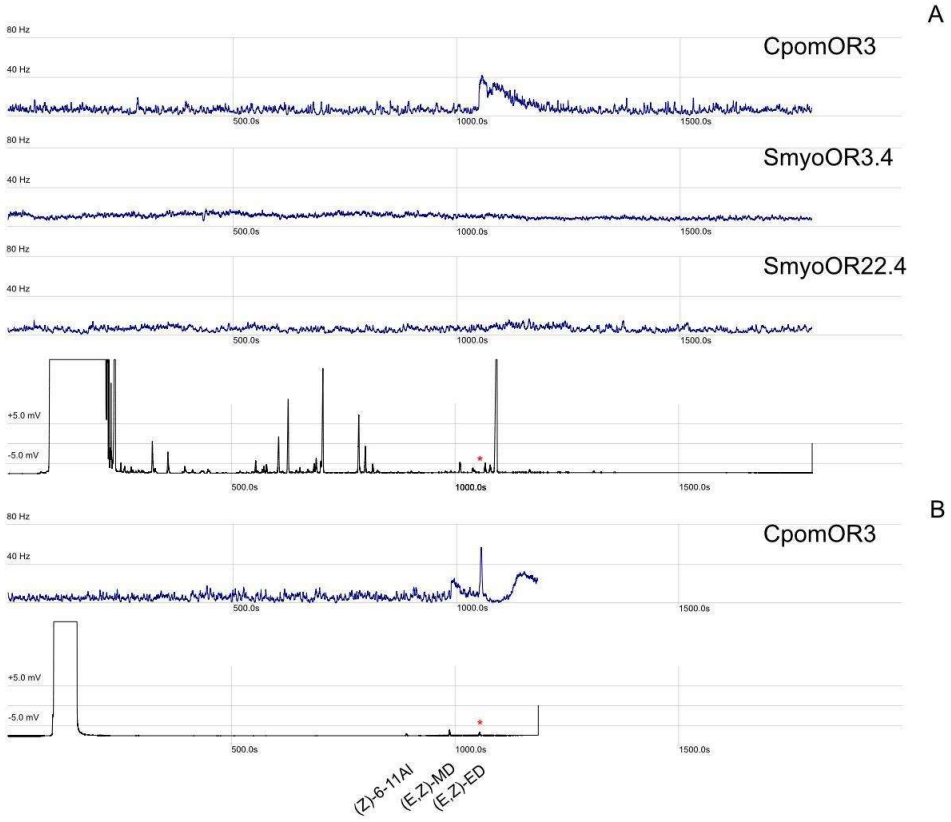

Figure 5. GC-SSR analysis of headspace. (**A**) Example from the headspace effects when testing the headspace Hoplomalus 562 from our previous study [29] on transgenic *Drosophila* expressing CpomOR3 (N = 11), SmyoOR3.4 (N = 3), and SmyoOR22.4 (N = 4). Red asterisk denotes the peak that possibly correlates with pear ester as in B. (**B**) Comparison with authentic samples testing the same CpomOR3 insect from A with the blend of (Z)-6-undecenal [Z6-11Al], methyl-E,Z-2,4 decadienoate [(E,Z)-MD], and ethyl-E,Z-2,4 decadienoate [(E,Z)-ED] 5.0 µg/µL. Below: the GC spectrum indicated peaks associated with 5.0 ng doses (GC 10 mV). Frequency plot (SSR 80 Hz) represents ab3A spikes per second, set with a Bin width of 100 ms seconds and a smooth filter line with 25 Taps. Note: both (E,Z)-MD and (E,Z)-ED enhance increment in the CpomOR3 spike frequency. Note: recordings from Figure 5 have been performed the same day (6 December 2019) using exactly the same headspace vial.

3.5. Structural Analysis

Upon alignment, the comparison of *S. myopaeformis* OR subunits with the respective CpomORs yielded the following identities/similarities: SmyoOR3.4, 0.409/0.595; SmyoOR3.3, 0.244/0.437; SmyoOR3.2, 0.054/0.188; SmyoOR3.1, 0.084/0.222; SmyoOR22.4, 0.33/0.55; SmyoOR22.3, 0.33/0.53; SmyoOR22.2, 0.34/0.56; and SmyoOR22.1, 0.34/0.57—Similarity Matrix: BLOSUM62). Alignment unveiled the most conserved regions in proximity to TM5 and TM6 for OR3 subunits and in proximity to the C-terminus for OR22 subunits (Figure 6A). Several conserved residues have been identified in proximity to the candidate ICL-3 hotspot for binding energy, including a tryptophan residue that has been demonstrated to be conserved among sequences of all insect Orco and OR subunits [71,72]. When comparing OR3 subunits, SmyoOR3.4 presented a shorter N-terminus and a gap in

the ICL-2; the latter feature was also observed for SmyoOR3.2. When comparing OR22 subunits, we observed a longer N-terminus for CpomOR22.

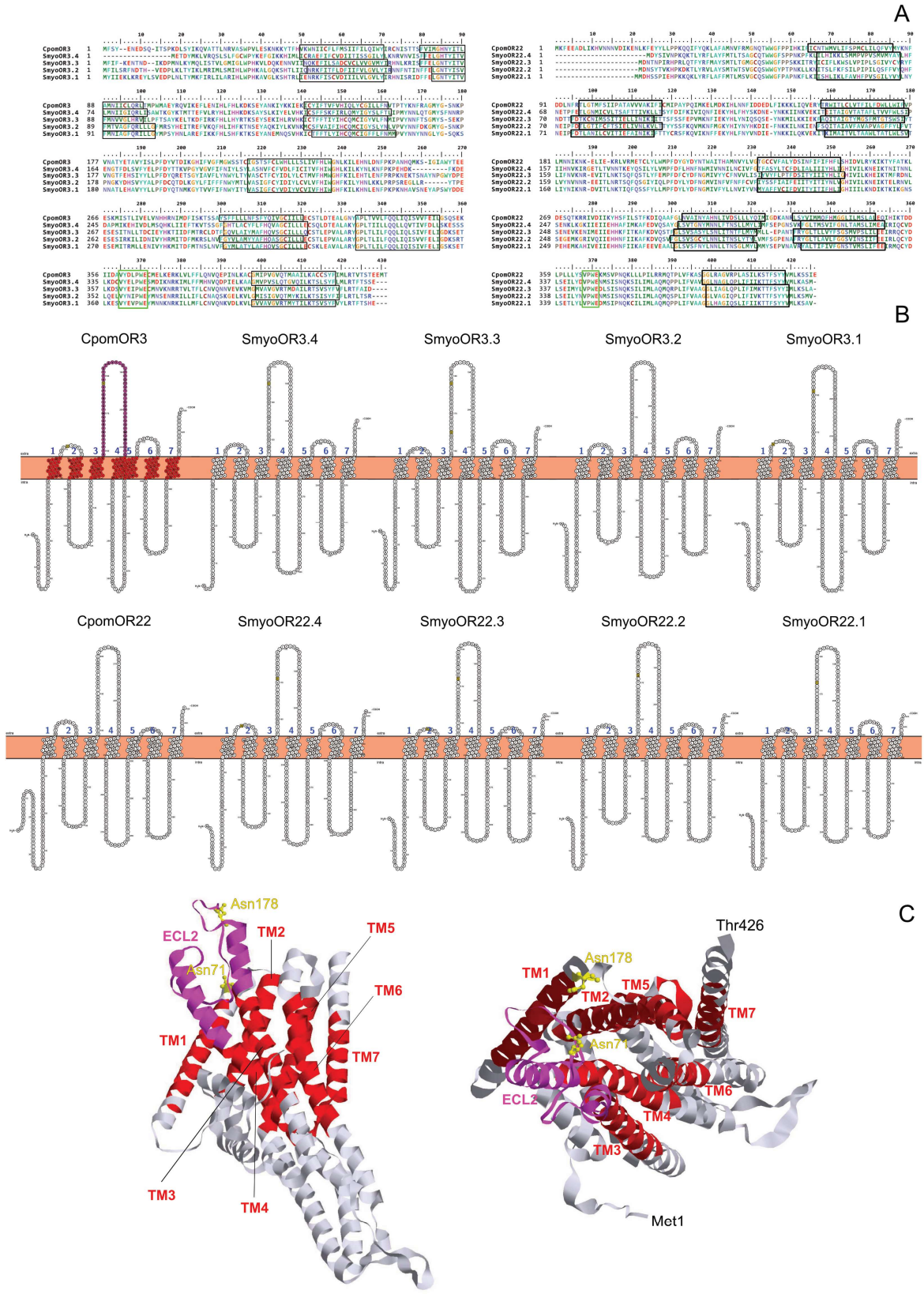

Figure 6. Polypeptide sequence and structural analysis. (**A**) polypeptide sequence alignment of the *C. pomonella* CpomOR3 (left) and CpomOR22 (right) with the respective *S. myopaeformis* subunits.

Black squares: transmembrane domains; green square: conserved region in proximity of the ICL-3 hotspot [71,72]. (**B**) Snake-plot analysis of OR3 (above) and OR22 (below) subunits. Yellow: asparagine amino acids predicted to host N-glycosylation motifs. (**C**) vertical view (left) and the transversal view (right) from the 3D analysis based on CpomOR3 highlighting transmembrane domains (TM1-TM7, red ribbons) and ICL-2 (magenta) containing the potential N-glycosylation site (asparagine, yellow); colours have been adopted as indicated in B; Met1 and Thr426 are labelled as the first (N-terminal) and the last (C-terminal) residues.

Analysing OR3 subunits, the snake-plot membrane topology resulted in a generally homogeneous length of ICLs 1 and 3, and ECLs 1, 2 and 3, but inhomogeneous lengths for N- and C-terminal domains, and for the ICL2 domain. Contrarily, OR22 subunits seem to maintain an overall homogeneous length among the various domains (Figure 6B). The snake plot analysis unveiled asparagine residues hosting potential N-glycosylations between the ECLs 1 and 2 for both OR3 and OR22 subunits, which are not present in SmyoOR3.2 and in CpomOR22. The 3D analysis of the CpomOR3-model unveiled the ICL-2 asparagine extending within the extracellular pocket formed by the loose packing of helices TM1–TM6 (Figure 6C).

4. Discussion

Odorant receptors of the red-belted clearwing moth *Synanthedon myopaeformis*, and of any moth of the Sesiidae family of Lepidoptera, have not, to our knowledge, been previously studied. The transcriptomic analysis of *S. myopaeformis* male antennae revealed that at least 62 OR genes were expressed, potentially encoding 65 proteins. These findings are comparable to our observations for the antennal OR capacity of the codling moth [27], wherein at least 58 ORs were identified as expressed, as in other moths [73]. Among the ORs of *S. myopaeformis,* we focused on those that clustered phylogenetically within the canonical pheromone receptor clade. Intriguingly, relative to the codling moth, SmyoORs in this clade were identified as part of subfamilies only within the CpomOR3 and CpomOR22 lineages. Despite the fact that CpomOR22 displays a strong female antennae bias [27,29,74], five candidate OR22 paralogues were identified as expressed in *S. myopaeformis* male antennae, revealing distinct evolutionary patterns of expression for genes within this subfamily.

The heterologous expression of eight OR subunits from *S. myopaeformis* in transgenic *D. melanogaster* unveiled responses to various compounds, including both insect pheromones and apple-emitted kairomones. Two of these OR subunits presented a shared pattern of activation among several ligands: SmyoOR3.4 unveiled evident responses mostly when exposed to unsaturated aldehydes and esters; SmyoOR22.4 reported wider activation responding to alcohols, aldehydes, esters, acetates, sesquiterpenes, as well as a cyanide (2-phanylacetonitrile) and a hydrazine (DMNT) (Figure 3B, Table 1, Supplementary Data File S3). Other subunits presented a limited activation (SmyoOR3.1, SmyoOR3.3, and SmyoOR22.1), and one resulted in the absence of any response to tested compounds (SmyoOR22.3), while SmyoOR3.2 and SmyoOR22.2 did not show evident ab3A spiking (Figure 3A). For SmyoOR3.2 and SmyoOR22.2, additional studies may help clarify whether these ORs are truly functional or not, since the absence of their spiking suggests that they are simply not expressed in the transgenic flies that we have used, despite that all of the SmyoOR genes from this study were synthesised with the *D. melanogaster* codon usage (see methods). Updated *D. melanogaster* lines expressing these subunits into CRISPR-gene-edited empty ab3As [75] are now deposited in the Bloomington *Drosophila* Stock Center (BDSC #98396 and #98399) and are available for further attempts. Alternatively, future projects may attempt to express these subunits ex novo, when more efficient expression methods will be available.

Investigating the dose–response characteristics of SmyoOR3.4 demonstrated that the pear ester ethyl-(E,Z)-2,4-decadienoate, renowned as one of the main esters emitted by Barlett pears [76] and apples [35], is the main agonist of this OR, which is in accordance with our previous findings from its activation of the CpomOR3 orthologue of *C. pomonella* [28,60]. Like CpomOR3, SmyoOR3.4 also responds to the methyl ester (methyl-(E,Z)-2,4-decadienoate), despite that this ligand acts as a partial agonist (Figure 4A). Hill coefficients of pear and methyl esters from the dose–response analysis resulted in values higher than 1.0 [(E,Z)-MD > (E,Z)-ED > 1.0], suggesting, hypothetically, that SmyoOR3.4 binds to multiple molecules of these two ligands [77]. In addition, SmyoOR3.4 responds to the unsaturated aldehyde (Z)-6-undecenal that we have reported among the main agonists of the *C. pomonella* OR22 [29]. Interestingly, when compared with hexane, pear and methyl esters also unveiled a significant spiking when they were tested on SmyoOR22.4.

The plant-volatile pear ester is among the main attractants of the codling moth [30]; however, monitoring programs for *C. pomonella* using traps baited with this kairomone also enabled the remote detection of other pest species, among which *S. myopaeformis* was identified as one of the main species attracted [34,78], suggesting similar chemosensory systems with the codling moth. In addition, as shown for *C. pomonella* [79], the pear ester evokes evident antennal electrophysiological activity on both females and males of *S. myopaeformis*, providing the highest responses on female antennae [34]. Analysing the response spectrum of SmyoOR22.4, we identified significant effects by several apple-emitted ligands that have been previously reported to be active on the chemosensory systems of *C. pomonella* [59]. These ligands included (R/S)-linalool, (Z)-3-hexenol, nonanal, hexyl 2-methyl-butanoate, methyl salicylate, (E)-β-farnesene, (E,E)-α-farnesene, (E)-β-caryophyllene, and 2-(2,2-Dimethylhydrazino)-4-(5-nitro-2-furyl)thiazole (DMNT), among which some are also active on SmyoOR3.4 (Figure 3B). Furthermore, SmyoOR22.4 shows significant effects by (E,E)-alpha-farnesol, an alcohol detected in trace quantities from emissions by Granny Smith apples [80], which we have recently demonstrated as an inhibitor of the CpomOR22 orthologue from the codling moth [29]. In addition, SmyoOR22.4 showed significant effects when tested by the main pheromone of *S. myopaeformis* (Z,Z)-3,13-Octadecadien-1-yl acetate [81], the main pheromone of the codling moth (E,E)-8,10-dodecadien-1-ol [82–84], and the codlemone agonist, (E,E)-8,10-dodecadien-1-yl acetate, which is renowned as the main pheromone of other tortricid moths [85–89]. While speculative, a possible explanation of the existence of a receptor in *S. myopaeformis* dedicated to the detection of pheromones from other moths may be of trophic importance, since these moths share the same host range, facilitating host finding for *S. myopaeformis*, or, eventually, aggregation with its conspecifics. On the other side, SSR screening unveiled (E,E)-8,10-dodecadien-1-ol inhibiting SmyoOR3.3 (Figure 3B), suggesting that, most possibly, more complex OR tuning behind the presence of codlemone may regulate species' recognition and/or discrimination.

Other ligands that we have found active on SmyoOR subunits are unsaturated aldehydes, including (Z)-4-undecenal, (Z)-6-undecenal, and (E,E)-2,4-decadienal, showing some of the most evident spiking effects on SmyoOR3.4 [3.17 ± 0.80; 4.46 ± 1.05; 2.14 ± 0.29 Δspikes/(0.5sec)*spike, respectively], while only (Z)-4-undecenal and (E,E)-2,4-decadienal were associated with significant spiking when tested on SmyoOR22.4 (Supplementary Data File S3). (Z)-4-undecenal has been part of our previous pharmacological investigations on the OR69a subunits of *D. melanogaster* [90] and *D. suzukii* [65], being identified among the aldehydes emitted from the autoxidation of *Drosophila*'s cuticular hydrocarbons. The activation of SmyoOR3.4 and SmyoOR22.4 by (Z)-4-undecenal is intriguing; however, to our knowledge, no ecological roles for (Z)-4-undecenal are yet renowned in association with the apple clearwing moth and other lepidopterans. Although possible, the SmyoORs' activation by(Z)-4-undecenal may result from its structural similarity

with other active aldehydes that may have ecological relevance for *S. myopaeformis* outside the scope of this study, assuming evidence of broad emissions of aldehyde ligands from diverse sources, ranging from plants and animals [91]. In accordance, our experimental records demonstrated the specificity of SmyoOR3.4 to (Z)-6-undecenal, for which SSR-screening reported it to be the most active, although adjusting for vapour pressure suggested this ligand as a partial agonist (Figure 4A). Despite this, the GC-SSR analysis of synthetic ligands (Figure 4B) demonstrated effects to (Z)-6-undecenal at doses proximal to 1.0 nanograms, while effects by pear and methyl esters were visible at doses not lower than 100 ng, suggesting (Z)-6-undecenal as a real SmyoOR3.4 agonist.

The unsaturated aldehyde 6-undecenal is among the main constituents from the essential oils of coriander (*Coriandrum sativum*), though it was not specified whether it was present either in the *E* or the *Z* isomer [92,93]; however, behavioural studies are necessary to demonstrate whether the unsaturated aldehydes that we have found active on SmyoOR3.4 are attractants or repellents for the apple clearwing moth. Despite this, evidence of the non-host origins of (Z)-4- and (Z)-6-undecanal and our reported findings of activity on ORs from other insect species including dipteran OR69As [65,90] and the *C. pomonella* OR22 [29] are compelling, and these findings are consistent with the idea that various insects' chemosensory receptor channels can be characterised by a somewhat common pharmacology [94–97].

Apart from the aforementioned aldehydes, other compounds associated with non-hosts have been found active on SmyoORs; these include 3-octanol, active on both SmyoOR3.4 and SmyoOR3.1, and 2-phenylethanol, citral, beta-cyclocitral, and 2-phenylacetonitrile, active on SmyoOR22.4. The reasons for which compounds that are non-host-emitted are active on *Synanthedon* OR subunits are unknown. However, this evidence, together with findings of the SmyoORs' activation by the unsaturated aldehydes, is consistent with insect chemosensory combinatorial coding as the primary coding mode of insect olfactory systems; while some olfactory receptors respond to unique (SmyoOR3.1), or few ligands (SmyoOR22.1), others may have a wider (SmyoOR3.4) or even the widest (SmyoOR22.4) spectrum of activators [19,98,99], facilitating tuning to numerous ligands to advance complex ecological functions.

The GC-SSR analysis of the apple headspace on transgenic *Drosophila melanogaster* expressing CpomOR3 demonstrated activation at a retention time, for which a comparison with active standards unveiled that it represents the pear ester (Figure 5). When tested on SmyoOR3.4 and SmyoOR22.4, none of the Hoplomalus/*Malus* apple headspace samples resulted in the activation of these subunits. As mentioned above, up to now, ethyl-(E,Z)-2,4-decadienoate, known as a pear ester, has been found among the emissions from Barlett pears [76] and apples [35], together with its methyl isomer and other short chain alcohol moieties of esters from E-2-Z-4-decadienoic acid. The pear ester serves as the main semiochemical across the various applications for the control and monitoring of the codling moth [30,31,33]. Despite our findings from SSR screening (Figure 3B) and dose–response experiments (Figure 4A) of the SmyoOR3.4 activation to this ligand, GC-SSR demonstrated that doses of this compound within the apple headspace are not capable of enhancing SmyoOR3.4 spiking (Figure 5A), which was rather achieved when the pure compound was injected at doses proximal to 10.0 ng (Figure 4B). Several studies have reported the coexistence of more than one chemosensory OR subunit in insect OSNs [90,100–103]. Others demonstrated the co-expression of Gustatory Receptors (GRs) and Ionotropic Receptors (IRs), together with ORs, within the same sensory neurons [104,105]. Expecting the coexistence of multiple cation channels on the dendrites of OSNs and, consequently, their possible cross-interactions, we cannot tell whether the SmyoORs that we have studied may be rather uniquely expressed within single OSNs or co-localised within the same neurons.

Taking a possible OR co-localization scenario, from the activation to the pear ester that we have observed solely for the SmyoOR3.4 subunit, and from the absence of the same effects for SmyoOR3.1, OR3.2, and OR3.3 subunits, we may hypothesize a structural rather than a functional role from the additional OR3s that may contribute to ligand sensing by forming functional ion channels with OR3.4. Among these ORs, when expressed in transgenic *Drosophila*, SmyoOR3.2 did not show evident ab3A spiking and did not respond to any ligand. Interestingly, the 3D analysis of OR3 unveiled the extension of an asparagine residue hosting possible N-glycosylation motifs within the extracellular pocket formed by the loose packing of helices TM1–TM6 (Figure 6), which Butterwick et al. [106] reported as a binding site for OR ligands. While we do not know whether the presence of this asparagine may somehow influence OR3/ligand binding, its absence in SmyoOR3.2, which is the sole non-functional candidate OR3 homologue (Figure 3), is compelling.

The absence of deposited 3D models for OR22 orthologues prevented us from adding 3D investigations to the polypeptide sequence and snake-plot analysis of the SmyoOR22s, further precluding the identification of key amino acids with hypothetical involvement in the receptors' functionality. Despite this, our data indicated SmyoOR22.4 to be the most active (Figure 3), apart from which only OR22.1 responded to (E)-β-caryophillene and β-cyclocitral. Although the scenario remains speculative, for these subunits, we may assume a similar case with the one encountered for OR3s, where additional OR22s subunits may add to ligand-sensing capacities of OR22.4 by forming heteromeric channels.

To our knowledge, there are no reports investigating the in situ expression of *S. myopaeformis* ORs on the antennal OSNs, and results from their functional co-expression are also lacking. Future studies on antennal neurons of *S. myopaeformis*, combined with testing transgenic *D. melanogaster* co-expressing the various SmyoORs within the same neurons, are needed to verify this hypothesis.

5. Conclusions

In this study, we have identified, isolated, and functionally characterised some key odorant receptors of the red-belted clearwing moth *S. myopaeformis*, conducting their heterologous expression in ab3A neurons of transgenic *D. melanogaster,* which we approached by SSR and GC-SSR. Among the ORs that we have tested, SmyoOR3.4 was the main sensor for the pear ester, although it showed a different pharmacology when compared with its orthologue from *C. pomonella*. Apart from SmyoOR3.4, we demonstrated a wide tuning to apple-emitted ligands for another OR, SmyoOR22.4, giving further evidence of some sort of chemosensory parallelism between *S. myopaeformis* and the codling moth, since the CpomOR22 orthologue from the latter also responds to the same ligands [29]. While the existence of such a chemosensory parallelism between two pest species sharing the same host may complicate this scenario, when attempting to motivate its ecological relevance, our evidence hypothetically suggests that insects infesting the same plants may be characterised by somewhat similar tuning modalities of their chemosensory systems. In such a context, apart from the pear ester [34], other semiochemicals that we have found active from this study, which are also detected by the codling moth [29,59], may represent additional molecular candidates to be integrated into alternative IPM strategies that can benefit both the control and monitoring programs of these two moths. The given paralogy of OR3 and OR22 in *Synanthedon* will inform future studies attempting the co-expression of these subunits for their further functional characterization in transgenic *Drosophila*. For these efforts, future studies will require the isolation and the GC-SSR testing of the headspace from apple barks in the presence or absence of the red-belted clearwing moth's infestation. It would be essential to validate the eventual emission of the pear ester or of the other ligands that we have found active on the aforementioned ORs from bark. In parallel, we

could make use of the CRISPR gene-editing protocols that have been optimised on the codling moth [68], to generate gene-edited *S. myopaeformis* knock-out lines for the aforementioned genes. These lines may help the investigation of mechanisms for pear ester sensing, eventually unveiling whether this sensing involves the activation of the other paralogues. Further behavioural trials may validate the activation of this pest insect by the other ligands that we have found active, among which, we have already identified the methyl ester and the unsaturated aldehyde (Z)-6-undecenal as partial agonists, representing additional candidates for ongoing semiochemical-based efforts toward the control of the red-belted clearwing moth.

Supplementary Materials: The following supporting information can be downloaded at: https://www.mdpi.com/article/10.3390/agriculture15101112/s1, Supplementary Table S1: Primer sequences used to amplify SmyoOR-CDSs, with their respective Tms. Supplementary Data File S1: Annotation of SmyoORs, indicating the ORF status (complete/incomplete), lengths, best hits based on orthologs from *C. pomonella* (Walker et al. [27]), and percentage of identity with the latter. Supplementary Data File S2: Polypeptide sequences of the ORs used in the phylogeny of this report. Supplementary Data File S3: Raw spike counting, spikes/second, and statistical analysis of ab3A neurons of *D. melanogaster* expressing SmyoOR subunits, testing the compound library from Table 1, and for the CpomOR3 subunit, testing Hoplomalus and *Malus* headspace. Asterisks and yellow marks denote compounds enhancing significant spiking based on Wilcoxon Signed Rank tests (SmyoORs) upon conducting tests of normality (Shapiro–Wilk, $\alpha = 0.05$). For comparative reasons, given the inconsistencies of a Shapiro–Wilk's p-value < 0.05, the same data have been also analysed by a parametric statistical analysis (paired t-test). Paired t-test was used to validate significant differences from the solvent's effect when flies expressing CpomOR3 were tested by GC-SSR. In this file, "i" depicts evidence of an inhibitory effect that we observed from (E,E)-8,10-dodecadien-1-ol when it was tested on SmyoOR3.3. Note: for CpomOR3, not all of the headspace samples show activity at the RT 1055 sec, indicating the absence in some cases of the respective active ligand in the headspace. Supplementary Data File S4: Raw, corrected, and normalised data from dose–response experiments testing SmyoOR3.4 to (Z)-6-undecenal, ethyl-(E,Z)-2,4-decadienoate (pear ester), and methyl (E,Z)-2,4-decadienoate (methyl ester). Note: effects to pear ester and methyl ester were corrected for vapour pressure, taking (Z)-6-undecenal as the standard. Dose–response values were used to plot data, as shown in Figure 2. Supplementary Data File S5: Whole Transcriptome Metrics, including Length Statistics and Composition and BUSCO results. Supplementary Data File S6: Expression data indicated as FPKM values and Log_2(FPKM), sorted by names (as in Supplementary Data File S4) and sorted by expression (as in Figure 2) of the SmyoORs identified from the transcriptomic analysis of this study. Supplementary Figure S1: Headspace from Hoplomalus and *Malus* extracts tested on different insects expressing SmyoOR3.4 (N = 3) and SmyoOR22.4 (N = 3). We observed an overall absence of effects: the apparent increment in spike counting was not confirmed performing further recordings. Note: SmyoOR22.4 was also tested on a headspace from *Hanseniospora uvarum* (headspace DP22) which was part of a previous investigation [65].

Author Contributions: A.M.C. and W.B.W.III conceived and designed the experiments. W.B.W.III performed genomic, transcriptomic, and phylogenetic analyses that led to the identification and characterization of SmyoOR transcripts, which he isolated and cloned to generate transgenic fly lines. A.M.C. performed SSR, dose–response experiments, GC-SSR, data analysis, statistical analysis, and structural analysis. The first draft of the manuscript was written by A.M.C. and both authors commented on previous versions of the manuscript. A.M.C. and W.B.W.III read, finalised, and approved the manuscript. All authors have read and agreed to the published version of the manuscript.

Funding: Open-access funding provided by the Swedish University of Agricultural Sciences. SSR studies were performed in the frame of the Crafoordska Stiftelsen project number 20180954, title: "*Control of apple pests with fruit and yeast odorants*". Running costs for SSR experiments were covered by the research unit Chemical Ecology-Horticulture (Department of Plant Protection Biology, SLU-Alnarp) and by Lars Hiertas Minne Grant N. FO2018-0209, title: "*Control of apple pest insects with fruit-*

and yeast-odorants". GC-SSR studies, data analysis, and manuscript preparation were undertaken in the course of the FORMAS Swedish research council project number 2018-00891, title "*Control of fruit pests by targeting larval chemical sensing*".

Institutional Review Board Statement: This study did not require institutional review board approval because it did not involve human subjects or animals, the use of which can be construed as having possible ethical issues.

Data Availability Statement: Data will be made available on request by writing to the corresponding author.

Acknowledgments: We thank Júlia Katalin Jósvai (Plant Protection Institute, Hungarian Research Network, Center for Agricultural Research (HUN-REN CAR)) for assistance with trapping, collecting, and dissecting *S. myopaeformis* specimens. The authors acknowledge support from Science for Life Laboratory, the National Genomics Infrastructure (NGI), and Uppmax for providing computational infrastructure. The use or mention of trade names and products herein does not represent an endorsement by the USDA. The USDA is an equal opportunity provider and employer. This manuscript is part of the research topic: "*Chemosensory-Based Pest Management of Insects and Other Protostomes in Crop Protection*". We thank the MDPI Agriculture Editorial Board for supporting our submission.

Conflicts of Interest: The authors declare that they have no known competing financial interests or personal relationships that could have appeared to influence the work reported in this paper.

References

1. Dickler, E. Zur Biologie und Schadwirkung von *Synanthedon myopaeformis* Brkh. (Lepid., Aegeriidae), einem neuen Schädling in Apfeldichtpflanzungen. *Z. Angew. Entomol.* **1976**, *82*, 259–266. [CrossRef]
2. Warner, J.; Hay, S. Observation, monitoring, and control of clearwing borers (Lepidoptera: Sesiidae) on apple in central Ontario. *Can. Entomolol.* **1985**, *117*, 1471–1478. [CrossRef]
3. Bergh, J.C.; Leskey, T.C. Biology, ecology, and management of dogwood borer in eastern apple orchards. *Can. Entomolol.* **2003**, *135*, 615–635. [CrossRef]
4. Ateyyat, M.A. Efficacy of some insecticides against the small red-belted clearwing borer, *Synanthedon myopaeformis* (Borkh.) (Lepidoptera: Sessiidae), in apple orchards in Jordan. *Commun. Agric. Appl. Biol. Sci.* **2005**, *70*, 759–765.
5. Trematerra, P. On the possibility of mass-trapping *Synanthedon myopaeformis* Bkh. (Lep., Sesiidae). *J. Appl. Entomol.* **1993**, *115*, 476–483. [CrossRef]
6. Balázs, K.; Bujáki, G.; Farkas, K. Incorporation of apple clearwing (*Synanthedon myopaeformis* Bork.) control into the IPM system of apple. *Acta Hortic.* **1996**, *422*, 134–139. [CrossRef]
7. Judd, G.J.R.; Bedford, K.; Cossentine, J. Control of Apple Clearwing Moth, *Synanthedon myopaeformis*, with Tree-trunk Applications of Reduced-risk Insecticides, Nematodes and Barriers. *J. Entomol. Soc. Br. Columbia* **2015**, *112*, 69–83. [CrossRef]
8. El-Ashry, R.M.; El-Sheikh, M.F.M.; Azazi, A.M.; Olphat, E.A. Field Control of *Synanthedon myopaeformis* Borkh and Zeuzera pyrina L. Using Entomopathogenic Nematodes, Insecticides and Microbial Agents. *Egypt. J. Agronematol.* **2018**, *17*, 121–131. [CrossRef]
9. Erler, F. Efficacy of tree trunk coating materials in the control of the apple clearwing, *Synanthedon myopaeformis*. *J. Insect Sci.* **2010**, *10*, 63. [CrossRef]
10. Ateyyat, M.A. Effect of three apple rootstocks on the population of the small red-belted clearwing borer, *Synanthedon myopaeformis*. *J. Insect Sci.* **2006**, *6*, 40. [CrossRef]
11. Witzgall, P.; Stelinski, L.; Gut, L.; Thomson, D. Codling moth management and chemical ecology. *Ann. Rev. Entomol.* **2008**, *53*, 503–522. [CrossRef] [PubMed]
12. Tumlinson, J.H.; Yonce, C.E.; Doolittle, R.E.; Heath, R.R.; Gentry, C.R.; Mitchell, E.R. Sex pheromones and reproductive isolation of the lesser peachtree borer and the peachtree borer. *Science* **1974**, *185*, 614–616. [CrossRef]
13. Voerman, S.; Minks, A.K.; Van Wetswinker, G.; Tumlinson, J.H. Activity of 3,13-octadecadien-1-ol acetates to the male clearwing moth *Synanthedon myopaeformis* (Borkhausen) (Lepidoptera, Sesiidae). *Entomol. Exp. Applicata* **1978**, *23*, 301–304. [CrossRef]
14. Szöcs, G.; Tóth, M.; Sziráki, G.Y.; Schwarz, M. 2,13- and 3,13-octadecadienyl compounds composing sex attractants for tineid and sesiid moths (Lepidoptera). *Biochem. Syst. Ecol.* **1989**, *17*, 417–422. [CrossRef]
15. El-Sayed, A.M. The Pherobase: Database of Insect Pheromones and Semiochemicals [Online]. 2009. Available online: http://www.pherobase.com (accessed on 28 March 2024).
16. Vogt, R.G. Molecular Basis of Pheromone Detection in Insects. In *Comprehensive Insect Physiology, Biochemistry, Pharmacology and Molecular Biology*; Gilbert, L.I., Iatro, K., Gill, S., Eds.; Vol. 3 Endocrinology; Elsevier: London, UK, 2005; pp. 753–804. [CrossRef]

17. Fleischer, J.; Krieger, J. Insect pheromone receptors—Key elements in sensing intraspecific chemical signals. *Front. Cell. Neurosci.* **2018**, *12*, 425. [CrossRef] [PubMed]
18. Sato, K.; Pellegrino, M.; Nakagawa, T.; Nakagawa, T.; Vosshall, L.B.; Touhara, K. Insect olfactory receptors are heteromeric ligand-gated ion channels. *Nature* **2008**, *452*, 1002–1006. [CrossRef]
19. Touhara, K.; Vosshall, L. Sensing odorants and pheromones with chemosensory receptors. *Annu. Rev. Physiol.* **2009**, *71*, 307–332. [CrossRef]
20. Wheelwright, M.; Whittle, C.R.; Riabinina, O. Olfactory systems across mosquito species. *Cell Tissue Res.* **2021**, *383*, 75–90. [CrossRef]
21. Montagne, N.; Chertemps, T.; Brigaud, I.; Francois, A.; Francois, M.C.; de Fouchier, A.; Lucas, P.; Larsson, M.C.; Jacquin-Joly, E. Functional characterization of a sex pheromone receptor in the pest moth *Spodoptera littoralis* by heterologous expression in *Drosophila*. *Eur. J. Neurosci.* **2012**, *36*, 2588–2596. [CrossRef]
22. de Fouchier, A.; Walker, W.B.; Montagne, N.; Steiner, C.; Binyameen, M.; Schlyter, F.; Chertemps, T.; Maria, A.; François, M.-C.; Monsempes, C.; et al. Functional evolution of Lepidoptera olfactory receptors revealed by deorphanization of a moth repertoire. *Nat. Commun.* **2017**, *8*, 15709. [CrossRef]
23. Dobritsa, A.A.; van der Goes van Naters, W.; Warr, C.G.; Steinbrecht, R.A.; Carlson, J.R. Integrating the molecular and cellular basis of odor coding in the *Drosophila* antenna. *Neuron* **2003**, *37*, 827–841. [CrossRef] [PubMed]
24. Hallem EAHo, M.G.; Carlson, J.R. The molecular basis of odor coding in the *Drosophila* antenna. *Cell* **2004**, *117*, 965–979. [CrossRef]
25. Brand, A.H.; Perrimon, N. Targeted gene expression as a means of altering cell fates and generating dominant phenotypes. *Development* **1993**, *118*, 401–415. [CrossRef] [PubMed]
26. Gonzalez, F.; Witzgall, P.; Walker, W.B. Protocol for heterologous expression of insect odourant receptors in *Drosophila*. *Front. Ecol. Evol.* **2016**, *4*, 24. [CrossRef]
27. Walker, W.B., III; Gonzalez, F.; Garczynski, S.; Witzgall, P. The chemosensory receptors of codling moth *Cydia pomonella*–expression in larvae and adults. *Sci. Rep.* **2016**, *6*, 23518. [CrossRef]
28. Bengtsson, J.M.; Gonzalez, F.; Cattaneo, A.M.; Montagné, N.; Walker, W.B.; Bengtsson, M.; Anfora, G.; Ignell, R.; Jacquin-Joly, E.; Witzgall, P. A predicted sex pheromone receptor of codling moth *Cydia pomonella* detects the plant volatile pear ester. *Front. Ecol. Evol.* **2014**, *2*, 33. [CrossRef]
29. Cattaneo, A.M.; Kwadha, C.A.; Pullmann-Lindsley, H.; Erdei, A.L.; Pitts, R.J.; Walker, W.B., III. Functional Characterization of a Female-Biased Chemoreceptor of the Codling Moth (*Cydia pomonella*) Responding to Aldehydes and Other Volatile Compounds. *J. Chem. Ecol.* **2025**, *51*, 28. [CrossRef]
30. Light, D.M.; Knight, A.L.; Henrick, C.A.; Rajapaska, D.; Lingren, B.; Dickens, J.C.; Reynolds, K.M.; Buttery, R.G.; Merrill, G.; Roitman, J.; et al. A pear-derived kairomone with pheromonal potency that attracts male and female codling moth, *Cydia pomonella* (L.). *Naturwissenschaften* **2001**, *88*, 333–338. [CrossRef]
31. Light, D.M.; Knight, A.L. Specificity of codling moth (Lepidoptera: Tortricidae) for the host plant kairomone, ethyl (2E,4Z)-2,4-decadienoate: Field bioassays with pome fruit volatiles, analogue, and isomeric compounds. *J. Agric. Food Chem.* **2005**, *53*, 4046–4053. [CrossRef]
32. Tóth, M.; Jósvai, J.; Hári, K.; Pénzes, B.; Vuity Zs Holb, I.; Szarukán, I.; Kecskés Zs Dorgán-Zsuga, I.; Koczor, S.; Voigt, E. Pear ester based lures for the codling moth *Cydia pomonella* L.—A summary of research efforts in Hungary. *Acta Phytopathol. Entomol. Hung.* **2014**, *49*, 37–47. [CrossRef]
33. Knight, A.L.; Preti, M.; Basoalto, E.; Mujica, V.; Favaro, R.; Angeli, S. Combining female removal with mating disruption for management of *Cydia pomonella* in apple. *Entomol. Gen.* **2022**, *42*, 309–321. [CrossRef]
34. Tóth, M.; Landolt, P.; Szarukán, I.; Szólláth, I.; Vitányi, I.; Pénzes, B.; Hári, K.; Katalin Jósvai, J.; Koczor, S. Female-targeted attractant containing pear ester for *Synanthedon myopaeformis*. *Entomol. Exp. Appl.* **2012**, *142*, 27–35. [CrossRef]
35. Erdei, A.L.; Sousa, M.; Gonzalez, F.; Bengtsson, M.; Witzgall, P. Host Plant Odour and Sex Pheromone are Integral to Mate Finding in Codling Moth. *J. Chem. Ecol.* **2025**, *51*, 13. [CrossRef] [PubMed]
36. Cock, P.J.; Fields, C.J.; Goto, N.; Heuer, M.L.; Rice, P.M. The Sanger FASTQ file format for sequences with quality scores, and the Solexa/Illumina FASTQ variants. *Nucleic Acids Res.* **2010**, *38*, 1767–1771. [CrossRef]
37. Walker, W.B., III; Mori, B.A.; Cattaneo, A.M.; Gonzalez, F.; Witzgall, P.; Becher, P.G. Comparative transcriptomic assessment of the chemosensory receptor repertoire of *Drosophila suzukii* adult and larval olfactory organs. *Comp. Biochem. Physiol. Part D Genom. Proteom.* **2023**, *45*, 101049. [CrossRef]
38. Grabherr, M.G.; Haas, B.J.; Yassour, M.; Levin, J.Z.; Thompson, D.A.; Amit, I.; Adiconis, X.; Fan, L.; Raychowdhury, R.; Zeng, Q.; et al. Full-length transcriptome assembly from RNA-Seq data without a reference genome. *Nat. Biotechnol.* **2011**, *29*, 644–652. [CrossRef]
39. Li, B.; Dewey, C.N. RSEM: Accurate transcript quantification from RNA-Seq data with or without a reference genome. *BMC Bioinform.* **2011**, *12*, 323. [CrossRef]

40. Li, W.; Godzik, A. Cd-hit: A fast program for clustering and comparing large sets of protein or nucleotide sequences. *Bioinformatics* **2006**, *22*, 1658–1659. [CrossRef]
41. Seppey, M.; Manni, M.; Zdobnov, E.M. BUSCO: Assessing genome assembly and annotation completeness. In *Gene Prediction: Methods and Protocols*; Humana: New York, NY, USA, 2019; pp. 227–245. [CrossRef]
42. Waterhouse, R.M.; Seppey, M.; Simão, F.A.; Zdobnov, E.M. Using BUSCO to assess insect genomic resources. In *Insect Genomics: Methods and Protocols*; Humana Press: New York, NY, USA, 2019; pp. 59–74. [CrossRef]
43. Nishimura, O.; Hara, Y.; Kuraku, S. gVolante for standardizing completeness assessment of genome and transcriptome assemblies. *Bioinformatics* **2017**, *33*, 3635–3637. [CrossRef]
44. Camacho, C.; Coulouris, G.; Avagyan, V.; Ma, N.; Papadopoulos, J.; Bealer, K.; Madden, T.L. BLAST+: Architecture and applications. *BMC Bioinform.* **2009**, *10*, 421. [CrossRef]
45. Artimo, P.; Jonnalagedda, M.; Arnold, K.; Baratin, D.; Csardi, G.; De Castro, E.; Duvaud, S.; Flegel, V.; Fortier, A.; Gasteiger, E.; et al. ExPASy: SIB bioinformatics resource portal. *Nucleic Acids Res.* **2012**, *40*, W597–W603. [CrossRef] [PubMed]
46. Sievers, F.; Wilm, A.; Dineen, D.; Gibson, T.J.; Karplus, K.; Li, W.; Lopez, R.; McWilliam, H.; Remmert, M.; Söding, J.; et al. Fast, scalable generation of high-quality protein multiple sequence alignments using Clustal Omega. *Mol. Syst. Biol.* **2011**, *7*, 539. [CrossRef]
47. Haas, B.J.; Papanicolaou, A.; Yassour, M.; Grabherr, M.; Blood, P.D.; Bowden, J.; Couger, M.B.; Eccles, D.; Li, B.O.; Lieber, M.; et al. De novo transcript sequence reconstruction from RNA-seq using the Trinity platform for reference generation and analysis. *Nat. Protoc.* **2013**, *8*, 1494–1512. [CrossRef]
48. Langmead, B.; Trapnell, C.; Pop, M.; Salzberg, S.L. Ultrafast and memory-efficient alignment of short DNA sequences to the human genome. *Genome Biol.* **2009**, *10*, R25. [CrossRef] [PubMed]
49. Li, H.; Handsaker, B.; Wysoker, A.; Fennell, T.; Ruan, J.; Homer, N.; Marth, G.; Abecasis, G.; Durbin, R.; 1000 Genome Project Data Processing Subgroup. The sequence alignment/map format and SAMtools. *Bioinformatics* **2009**, *25*, 2078–2079. [CrossRef] [PubMed]
50. Briscoe, A.D.; Macias-Munoz, A.; Kozak, K.M.; Walters, J.R.; Yuan, F.R.; Jamie, G.A.; Martin, S.H.; Dasmahapatra, K.K.; Ferguson, L.C.; Mallet, J.; et al. Female Behaviour Drives Expression and Evolution of Gustatory Receptors in Butterflies. *PLoS Genet.* **2013**, *9*, e1003620. [CrossRef]
51. Wanner, K.W.; Anderson, A.R.; Trowell, S.C.; Theilmann, D.A.; Robertson, H.M.; Newcomb, R.D. Female-biased expression of odourant receptor genes in the adult antennae of the silkworm, *Bombyx mori*. *Insect Mol. Biol.* **2007**, *16*, 107–119. [CrossRef]
52. Walker, W.B., III; Cattaneo, A.M.; Stout, J.L.; Evans, M.L.; Garczynski, S.F. Chemosensory Receptor Expression in the Abdomen Tip of the Female Codling Moth, *Cydia pomonella* L. (Lepidoptera: Tortricidae). *Insects* **2023**, *14*, 948. [CrossRef]
53. Walker, W.B., III; Roy, A.; Anderson, P.; Schlyter, F.; Hansson, B.S.; Larsson, M.C. Transcriptome Analysis of Gene Families Involved in Chemosensory Function in *Spodoptera littoralis* (Lepidoptera: Noctuidae). *BMC Genom.* **2019**, *20*, 428. [CrossRef]
54. Katoh, K.; Rozewicki, J.; Yamada, K.D. MAFFT online service: Multiple sequence alignment, interactive sequence choice and visualization. *Brief. Bioinform.* **2019**, *20*, 1160–1166. [CrossRef]
55. Guindon, S.; Dufayard, J.F.; Lefort, V.; Anisimova, M.; Hordijk, W.; Gascuel, O. New algorithms and methods to estimate maximum-likelihood phylogenies: Assessing the performance of PhyML 3.0. *Syst. Biol.* **2010**, *59*, 307–321. [CrossRef] [PubMed]
56. Lefort, V.; Longueville, J.E.; Gascuel, O. SMS: Smart Model Selection in PhyML. *Mol. Biol. Evol.* **2017**, *34*, 2422–2424. [CrossRef] [PubMed]
57. Anisimova, M.; Gascuel, O. Approximate likelihood-ratio test for branches: A fast, accurate, and powerful alternative. *Syst. Biol.* **2006**, *55*, 539–552. [CrossRef]
58. Kumar, S.; Stecher, G.; Peterson, D.; Tamura, K. MEGA-CC: Computing core of molecular evolutionary genetics analysis program for automated and iterative data analysis. *Bioinformatics* **2012**, *28*, 2685–2686. [CrossRef]
59. Bengtsson, M.; Bäckman, A.-C.; Liblikas, I.; Ramirez, M.I.; Borg-Karlson, A.-K.; Ansebo, L.; Anderson, P.; Löfqvist, J.; Witzgall, P. Plant odor analysis of apple: Antennal response of codling moth females to apple volatiles during phenological development. *J. Agric. Food Chem.* **2001**, *49*, 3736–3741. [CrossRef]
60. Cattaneo, A.M.; Gonzalez, F.; Bengtsson, J.M.; Corey, E.A.; Jacquin-Joly, E.; Montagné, N.; Salvagnin, U.; Walker, W.B.; Witzgall, P.; Anfora, G.; et al. Candidate pheromone receptors of codling moth *Cydia pomonella* respond to pheromones and kairomones. *Sci. Rep.* **2017**, *7*, 41105. [CrossRef]
61. Gardette, M.; Alexakis, A.; Normant, J.F. Synthesis of (Z,Z)-3, 13-octadecadien-1-yl acetate component of the sex pheromone of *Synanthedon tenuis*. *J. Chem. Ecol.* **1983**, *9*, 225–233. [CrossRef] [PubMed]
62. Münch, D.; Galizia, C.G. DoOR: The Database of Odorant Responses. *ChemoSense* **2011**, *13*, 1–6.
63. Galizia, C.G.; Münch, D.; Strauch, M.; Nissler, A.; Ma, S. Integrating Heterogeneous Odor Response Data into a Common Response Model: A DoOR to the Complete Olfactome. *Chem. Senses* **2010**, *35*, 551–563. [CrossRef]
64. Bengtsson, M.; Liljefors, T.; Hansson, B.S.; Löfstedt, C.; Copaja, S.V. Structure-activity relationships for chain-shortened analogs of (Z)-5-decenyl acetate, a pheromone component of the turnip moth, *Agrotis segetum*. *J. Chem. Ecol.* **1990**, *16*, 667–684. [CrossRef]

65. Cattaneo, A.M.; Witzgall, P.; Kwadha, C.A.; Becher, P.G.; Walker, W.B., III. Heterologous expression and functional characterization of *Drosophila suzukii* OR69a transcript variants unveiled response to kairomones and to a candidate pheromone. *J. Pest Sci.* **2022**, *96*, 1149–1171. [CrossRef]
66. Pettersson, J.H.; Cattaneo, A.M. Heterologous investigation of metabotropic and ionotropic odorant receptors in ab3A neurons of *Drosophila melanogaster*. *Front. Mol. Biosci. Sec. Protein Biochem. Basic Appl. Sci.* **2024**, *10*, 1275901. [CrossRef]
67. Madeira, F.; Pearce, M.; Tivey, A.R.N.; Basutkar, P.; Lee, J.; Edbali, O.; Madhusoodanan, N.; Kolesnikov, A.; Lopez, R. Search and sequence analysis tools services from EMBL-EBI in 2022. *Nucleic Acids Res.* **2022**, *50*, W276–W279. [CrossRef]
68. Garczynski, S.F.; Martin, J.A.; Griset, M.; Willett, L.S.; Cooper, W.R.; Swisher, K.D.; Unruh, T.R. CRISPR/Cas9 Editing of the Codling Moth (Lepidoptera: Tortricidae) CpomOR1 Gene Affects Egg Production and Viability. *J. Econ. Entomol.* **2017**, *110*, 1847–1855. [CrossRef]
69. Tsirigos, K.D.; Peters, C.; Shu, N.; Kall, L.; Elofsson, A. The TOPCONS web server for consensus prediction of membrane protein topology and signal peptides. *Nucleic Acids Res.* **2015**, *43*, W401–W407. [CrossRef] [PubMed]
70. Omasits, U.; Ahrens, C.H.; Muller, S.; Wollscheid, B. Protter: Interactive protein feature visualization and integration with experimental proteomic data. *Bioinformatics* **2014**, *30*, 884–886. [CrossRef]
71. Bobkov, Y.V.; Walker, W.B.; Cattaneo, A.M. Altered functional properties of the codling moth Orco mutagenized in the intracellular loop-3. *Sci. Rep.* **2021**, *11*, 3893. [CrossRef] [PubMed]
72. Miller, R.; Tu, Z. Odorant receptor c-terminal motifs in divergent insect species. *J. Insect Sci* **2008**, *8*, 53. [CrossRef]
73. Montagné, N.; Wanner, K.; Jacquin-Joly, E. Olfactory genomics within the Lepidoptera. In *Insect Pheromone Biochemistry and Molecular Biology*; Academic Press: New York, NY, USA, 2021; pp. 469–505. [CrossRef]
74. Bengtsson, J.M.; Trona, F.; Montagné, N.; Anfora, G.; Ignell, R.; Witzgall, P.; Jacquin-Joly, E. Putative chemosensory receptors of the codling moth, *Cydia pomonella*, identified by antennal transcriptome analysis. *PLoS ONE* **2012**, *7*, e31620. [CrossRef]
75. Chahda, J.S.; Soni, N.; Sun, J.S.; Ebrahim, S.A.M.; Weiss, B.L.; Carlson, J.R. The molecular and cellular basis of olfactory response to tsetse fly attractants. *Chem. Senses* **2019**, *44*, E67–E68. [CrossRef]
76. Jennings, W.G.; Sevenants, M.R. Volatile Esters of Bartlett Pear III. *J. Food Sci.* **1964**, *29*, 123–240. [CrossRef]
77. Prinz, H. Hill coefficients, dose–response curves and allosteric mechanisms. *J. Chem. Biol.* **2010**, *3*, 37–44. [CrossRef] [PubMed]
78. Preti, M.; Favaro, R.; Knight, A.L.; Angeli, S. Remote monitoring of *Cydia pomonella* adults among an assemblage of nontargets in sex pheromone-kairomone-baited smart traps. *Pest Manag. Sci.* **2021**, *77*, 4084–4090. [CrossRef] [PubMed]
79. De Cristofaro, A.; Ioriatti, C.; Pasqualini, E.; Anfora, G.; Germinara, G.S.; Villa, M.; Rotundo, G. Electrophysiological responses of *Cydia pomonella* to codlemone and pear ester ethyl (E,Z)-2,4-decadienoate: Peripheral interactions in their perception and evidences for cells responding to both compounds. *Bull. Insectology* **2004**, *57*, 137–144.
80. Matich, A.J.; Rowan, D.D.; Banks, N.H. Solid phase microextraction for quantitative headspace sampling of apple volatiles. *Anal. Chem.* **1996**, *68*, 4114–4118. [CrossRef]
81. Vinczer, P.; Baán, G.; Novák, L.; Szántay, C. A novel stereocontrolled synthesis of (z,z)-3,13-octadecadien-1-yl acetate, the sex pheromone of *Synanthedon* species. *Tetrahedron Lett.* **1984**, *25*, 2701–2704. [CrossRef]
82. Roelofs, W.L.; Comeau, A.; Hill, A.; Milicevic, G. Sex attractant of the codling moth: Characterization with electroantennogram technique. *Science* **1971**, *174*, 297–299. [CrossRef]
83. Beroza, M.; Bierl, B.A.; Moffitt, H.R. Sex pheromones: (E8,E10)-Dodecadien-1-ol in the codling moth. *Science* **1974**, *183*, 89–90. [CrossRef]
84. McDonough, L.M.; Moffitt, H.R. Sex pheromone of the codling moth. *Science* **1974**, *183*, 978. [CrossRef]
85. Frérot, B.; Priesner, E.; Gallois, M. A sex attractant for the green budworm moth, *Hedya nubiferana*. *Z. Naturforsch.* **1979**, *34c*, 1248–1252. [CrossRef]
86. Roelofs, W.L.; Brown, R.L. Pheromones and evolutionary relationships of Tortricidae. *Ann. Rev. Ecol. Syst.* **1982**, *13*, 395–422. [CrossRef]
87. Davis, H.G.; McDonough, L.M.; Burditt, A.K.; Bieri-Leonhardt, B.A. Filbertworm sex pheromone. Identification and field tests of (E,E)- and (E,Z)-8,10 dodecadien-1-ol acetates. *J. Chem. Ecol.* **1984**, *10*, 53–61. [CrossRef] [PubMed]
88. Witzgall, P.; Chambon, J.P.; Bengtsson, M.; Unelius, C.R.; Appelgren, M.; Makranczy, G.; Muraleedharan, N.; Reed, D.W.; Hellrigl, K.; Buser, H.-R.; et al. Sex pheromones and attractants in the Eucosmini and Grapholitini (Lepidoptera, Tortricidae). *Chemoecology* **1996**, *7*, 13–23. [CrossRef]
89. Chambers, U.; Walton, V.M.; Mehlenbacher, S.A. Susceptibility of hazelnut cultivars to filbertworm, *Cydia latiferreana*. *Hortic. Sci.* **2011**, *46*, 1377–1380. [CrossRef]
90. Lebreton, S.; Borrero-Echeverry, F.; Gonzalez, F.; Solum, M.; Wallin, E.A.; Hedenström, E.; Hansson, B.S.; Gustavsson, A.L.; Bengtsson, M.; Birgersson, G.; et al. A *Drosophila* female pheromone elicits species-specific long-range attraction via an olfactory channel with dual specificity for sex and food. *BMC Biol.* **2017**, *15*, 88. [CrossRef]
91. Jumean, Z.; Gries, R.; Unruh, T.; Rowland, E.; Gries, G. Identification of the larval aggregation pheromone of Codling moth, *Cydia pomonella*. *J. Chem. Ecol.* **2005**, *31*, 911–924. [CrossRef] [PubMed]

92. Parthasarathy, V.; Chempakam, B.; Zachariah, T.J. *Chemistry of Spices*; CAB International: Oxfordshire, UK, 2008; ISBN 978-1-84593-405-7.
93. Rajeshwari, U.; Andallu, B. Medicinal benefits of coriander (*Coriandrum sativum* L.). *Spatula DD* **2011**, *1*, 51–58. [CrossRef]
94. Bobkov, Y.V.; Ache, B.W. Block by amiloride derivatives of odor-evoked discharge in lobster olfactory receptor neurons through action on a presumptive TRP channel. *Chem. Senses* **2007**, *32*, 149–159. [CrossRef]
95. Pask, G.M.; Bobkov, Y.V.; Corey, E.A.; Ache, B.W.; Zwiebel, L.J. Blockade of insect odorant receptor currents by amiloride derivatives. *Chem. Senses* **2013**, *38*, 221–229. [CrossRef]
96. Röllecke KWerner, M.; Ziemba, P.M.; Neuhaus, E.M.; Hatt, H.; Gisselmann, G. Amiloride derivatives are effective blockers of insect odorant receptors. *Chem. Senses* **2013**, *38*, 231–236. [CrossRef]
97. Bobkov, Y.V.; Corey, E.A.; Ache, B.W. An inhibitor of Na^+/Ca^{2+} exchange blocks activation of insect olfactory receptors. *Biochem. Biophys. Res. Commun.* **2014**, *450*, 1104–1109. [CrossRef] [PubMed]
98. Wyatt, T.D. *Pheromones and Animal Behavior: Chemical Signals and Signatures*; Cambridge University Press: New York, NY, USA, 2014. [CrossRef]
99. Andersson, M.N.; Löfstedt, C.; Newcomb, R.D. Insect olfaction and the evolution of receptor tuning. *Front. Ecol. Evol.—Chem. Ecol.* **2015**, *3*, 53. [CrossRef]
100. Robertsson, H.M.; Warr, C.G.; Carlson, J.R. Molecular evolution of the insect chemoreceptor gene superfamily in *Drosophila melanogaster*. *Proc. Natl. Acad. Sci. USA* **2003**, *100* (Suppl. S2), 14537–14542. [CrossRef]
101. Couto, A.; Alenius, M.; Dickson, B.J. Molecular, anatomical, and functional organization of the *Drosophila* olfactory system. *Curr. Biol.* **2005**, *15*, 1535–1547. [CrossRef]
102. Martin, F.; Boto, T.; Gomez-Diaz, C.; Alcorta, E. Elements of olfactory reception in adult *Drosophila melanogaster*. *Anat. Rec.* **2013**, *296*, 1477–1488. [CrossRef]
103. Münch, D.; Galizia, C.G. DoOR 2.0-Comprehensive mapping of *Drosophila melanogaster* odorant responses. *Sci. Rep.* **2016**, *6*, 21841. [CrossRef] [PubMed]
104. Task, D.; Lin, C.-C.; Vulpe, A.; Afify, A.; Ballou, S.; Brbic, M.; Schlegel, P.; Raji, J.; Jefferis, G.S.X.E.; Li, H.; et al. Chemoreceptor co-expression in *Drosophila melanogaster* olfactory neurons. *eLife* **2022**, *11*, e72599. [CrossRef]
105. Vulpe, A.; Menuz, K. Ir76b is a Co-receptor for Amine Responses in *Drosophila* Olfactory Neurons. *Front. Cell. Neurosci.* **2021**, *15*, 759238. [CrossRef]
106. Butterwick, J.A.; Del Mármol, J.; Kim, K.H.; Kahlson, M.A.; Rogow, J.A.; Walz, T.; Ruta, V. Cryo-EM structure of the insect olfactory receptor Orco. *Nature* **2018**, *560*, 447–452. [CrossRef]